Synthesis and Structure–Activity Relationships of EML4–ALK Inhibitors

December 2019

Kazuhiko IIKUBO

Synthesis and Structure–Activity Relationships of EML4–ALK Inhibitors

A Dissertation Submitted to
the School of the Integrative and Global Majors,
the University of Tsukuba
in Partial Fulfillment of the Requirements
for the Degree of Doctor of Philosophy in Medical Science
(Doctoral Program in Life Science Innovation)

Kazuhiko IIKUBO

This dissertation is described based on the following original articles.

- Discovery of *N*-{2-Methoxy-4-[4-(4-methylpiperazin-1-yl)piperidin-1-yl]phenyl}-*N'*-[2-(propane-2-sulfonyl)phenyl]-1,3,5-triazine-2,4-diamine (ASP3026), a Potent and Selective Anaplastic Lymphoma Kinase (ALK) Inhibitor

  Kazuhiko Iikubo, Yutaka Kondoh, Itsuro Shimada, Takahiro Matsuya, Kenichi Mori, Yoko Ueno, Minoru Okada

  Chemical and Pharmaceutical Bulletin, **2018**, *66*, 251–262.

- Synthesis and structure–activity relationships of pyrazine-2-carboxamide derivatives as novel echinoderm microtubule-associated protein-like 4 (EML4)–anaplastic lymphoma kinase (ALK) inhibitors

  Kazuhiko Iikubo, Kazuo Kurosawa, Takahiro Matsuya, Yutaka Kondoh, Akio Kamikawa, Ayako Moritomo, Yoshinori Iwai, Hiroshi Tomiyama, Itsuro Shimada

  Bioorganic & Medicinal Chemistry, **2019**, *27*, 1683–1692.

Abstract

Echinoderm microtubule-associated protein-like 4 (EML4)–anaplastic lymphoma kinase (ALK) is considered a valid therapeutic target for the treatment of EML4–ALK-positive non-small cell lung cancer (NSCLC). In this study, synthesis and structure–activity relationship (SAR) studies on 1,3,5-triazine derivatives and pyrazine-2-carboxamide derivatives were performed to identify novel EML4–ALK inhibitors.

In Chapter 1, I describe the synthesis and biological evaluation of 1,3,5-triazine derivatives. I also discuss the detailed SAR studies conducted on each structural component of 1,3,5-triazine derivative compounds using computational modeling. First, substituents at the 6-position of the 1,3,5-triazine ring were examined. SAR studies revealed that unsubstituted compound **12a** showed the most potent inhibitory activity against EML4–ALK among all compounds reported. Second, the SAR of the sulfonyl moiety of compound **12a** was investigated. These experiments revealed that the 2-isopropylsulfonyl derivative had the most potent inhibitory activity against EML4–ALK among all compounds reported. Third, substituent effects at the methoxy group of compound **12a** were examined. These experiments showed that the oxygen atom in the 2-methoxy group was important for the compound's inhibitory activity. Finally, optimization of the amine moiety revealed that compound **12a** exhibited the most promising *in vitro* profile among all compounds reported. The antitumor

activity of compound **12a** was evaluated in mice xenografted with NCI-H2228, human NSCLC tumor cells that endogenously express EML4–ALK. Oral administration of compound **12a** demonstrated dose-dependent antitumor activity and induced tumor regression.

In Chapter 2, I describe the synthesis and biological evaluation of pyrazine-2-carboxamide derivatives to identify a more potent EML4–ALK inhibitor with a different chemical structure to that of compound **12a**. I also discuss the detailed SAR studies conducted on each structural component of pyrazine-2-carboxamide derivative compounds using computational modeling. First, the substituent effects at the ethyl moiety of compound **30a** were examined. SAR studies revealed that the ethyl derivative **30a** showed the most potent inhibitory activity against EML4–ALK among all compounds reported. Next, optimization of the 3-(methanesulfonyl)anilino component of compound **30a** was performed. The docking model of compound **12a** with ALK indicated that the amine moiety of compound **12a** extends into the solvent-exposed region located outside the ATP-binding pocket. The docking model of **30a** suggested that the 3-(methanesulfonyl)anilino moiety of compound **30a** extends into the same region. Consistent with this observation, compound **35** retained inhibitory activity against EML4–ALK compared to that of compound **30a** (**30a**: IC_{50} = 17 nM, **35**: IC_{50} = 8.9 nM). Replacement of the 2-methoxy group of compound **35** with a 3-methoxy group enhanced the inhibitory activity (**37a**: IC_{50} = 0.37 nM). Finally, optimization of the amine moiety led to the discovery of compound **37c**. The antitumor activity of compound **37c** was evaluated in mice

xenografted with 3T3 cells expressing EML4–ALK. Once-daily oral administration of compound **37c** at a dose of 10 mg/kg for 5 days demonstrated 62% tumor regression, while compound **12a** showed 81% tumor growth inhibition.

Based on the two abovementioned studies, compounds **12a** and **37c** were identified as novel EML4–ALK inhibitors. In mice xenografted with 3T3 cells expressing EML4–ALK, the antitumor activity of compound **37c** was more potent than that observed for compound **12a**.

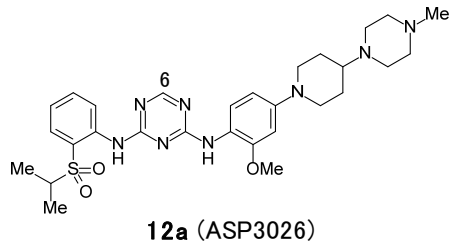

12a (ASP3026)

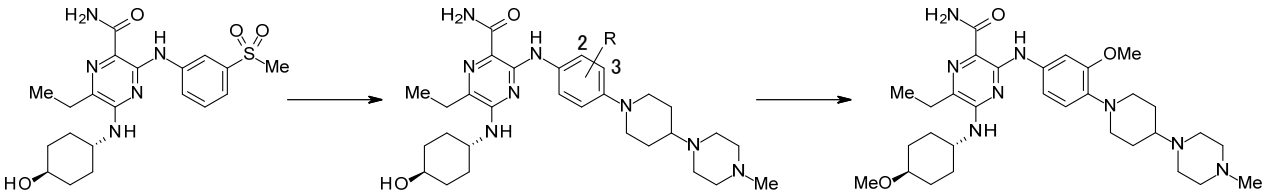

30a **35** : R = 2−MeO **37a** : R = 3−MeO **37c**

Contents

Abbreviations

A (amino acid)	alanine
AcOH	acetic acid
Ala (amino acid)	alanine
ALCL	anaplastic large-cell lymphoma
ALK	anaplastic lymphoma kinase
aq.	aqueous
Asp (amino acid)	aspartic acid
ATP	adenosine 5'-triphosphate
br (NMR)	broad peak
CI	chemical ionization
c-Pr	cyclopropyl
d (NMR)	doublet
DCE	1,2-dichloroethane
DCM	dichloromethane
dd (NMR)	doublet of doublets
DIPEA	*N*,*N*-diisopropylethylamine
DMF	*N*,*N*-dimethylformamide
DMI	1,3-dimethyl-2-imidazolidinone
DMSO	dimethyl sulfoxide
E (amino acid)	glutamic acid
EGFR	epidermal growth factor receptor
EI	electron ionization
EMAP	echinoderm microtubule-associated protein
EML4	echinoderm microtubule-associated protein-like 4
ESI	electrospray ionization
Et	ethyl

Et_2O	diethyl ether
EtOAc	ethyl acetate
EtOH	ethanol
FAB	fast atom bombardment
FDA	Food and Drug Administration
G (amino acid)	glycine
Glu (amino acid)	glutamic acid
Gly (amino acid)	glycine
h	hour(s)
HELP	hydrophobic EMAP-like protein
HPLC	high-performance liquid chromatography
HRMS	high resolution mass spectrum
IC_{50}	50% inhibitory concentration
i-Pr	isopropyl
JP2	Japanese Pharmacopoeia 2nd fluid
K (amino acid)	lysine
L (amino acid)	leucine
Leu (amino acid)	leucine
Lys (amino acid)	lysine
M (amino acid)	methionine
m (NMR)	multiplet
MC	methylcellulose
mCPBA	*m*-chloroperoxybenzoic acid
Me	methyl
MeCN	acetonitrile
MeOH	methanol
Met (amino acid)	methionine
min	minute(s)

MS	mass spectrum
MsOH	methanesulfonic acid
NBS	*N*-bromosuccinimide
NCS	*N*-chlorosuccinimide
n-hexane	normal hexane
NMP	1-methyl-2-pyrrolidone
NMR	nuclear magnetic resonance
NOD-SCID	non-obese diabetic-severe combined immunodeficiency
NPM	nucleophosmin
n-Pr	normal propyl
NSCLC	non-small cell lung cancer
PAMPA	parallel artificial membrane permeability assay
PPh_3	triphenylphosphine
q (NMR)	quartet
rt	room temperature
RTK	receptor tyrosine kinase
s (NMR)	singlet
SAR	structure–activity relationship
SCLC	small cell lung cancer
SEM	standard error of the mean
STAT3	signal transducer and activator of transcription 3
t (NMR)	triplet
THF	tetrahydrofuran
UPLC	ultra-performance liquid chromatography
Val (amino acid)	valine

General introduction

According to a report on cancer incidence and mortality statistics for major cancers in 20 regions throughout the world based on GLOBOCAN 2012, lung cancer remains the most common cancer in terms of both estimated new cases and estimated deaths [1]. Lung cancer is mainly classified into two types: non-small cell lung cancer (NSCLC) and small cell lung cancer (SCLC). The American Cancer Society reported that NSCLC is the most common type of lung cancer, accounting for approximately 80% to 85% of lung cancers [2]. Treatment for NSCLC depends mainly on the stage of the cancer and can include surgery, radiofrequency ablation, radiation therapy, chemotherapy, targeted therapy, immunotherapy and palliative procedures [2]. For example, surgery might be an option for early-stage NSCLC, radiation therapy might be used depending on the stage of the NSCLC and other factors, and chemotherapy may be recommended depending on the cancer's stage and other factors [2]. Among these options, molecular targeted cancer therapy based on a phenomenon known as oncogene addiction has emerged following accumulation of understanding of the genetic background, such as driver mutations and gene rearrangements [3, 4]. Epidermal growth factor receptor (*EGFR*) mutation and anaplastic lymphoma kinase (*ALK*) translocation, for example, are widely recognized genomic alterations observed in NSCLC [4].

ALK is a receptor tyrosine kinase (RTK) that belongs to the family of insulin RTKs [5,

6]. ALK was first identified as a nucleophosmin (*NPM*)–*ALK* fusion oncogene in anaplastic large-cell lymphoma (ALCL) [5]. Part of the *NPM* gene is fused to the portion of the *ALK* gene that contains the tyrosine kinase domain, resulting in NPM–ALK being constitutively active [6]. This type of chromosomal translocation involving ALK has been identified in several cancers, including NSCLC [7, 8, 9].

Echinoderm microtubule-associated protein-like 4 (*EML4*)–*ALK* fusion oncogene was identified in a subset of NSCLC patients in 2007 [10]. Human EML4 is a member of the echinoderm microtubule-associated protein (EMAP) family and is essential for microtubule formation [11]. Human EML4 contains the family-specific hydrophobic EMAP-like protein (HELP) domain located within the N-terminal region, and the WD repeat region located within the central and C-terminal region [11]. *EML4–ALK* variant 1 comprises the part of the *EML4* gene that contains the basic region, the HELP domain and the part of the WD repeat region that is fused to the intracellular region of the *ALK* gene that contains the tyrosine kinase domain (Figure 1) [10]. The EML4–ALK oncogenic fusion kinase plays an essential role in the pathogenesis of NSCLC [12]. In addition, EML4–ALK has constitutive tyrosine kinase activity [10,13]. A study previously reported that downstream signaling pathways may differ depending on the ALK fusion proteins present [13]. For example, signal transducer and activator of transcription 3 (STAT3) is likely to play a central role in NPM–ALK-mediated tumorigenesis, but is unlikely to play a major role in that involving EML4–ALK [7, 8, 13, 14].

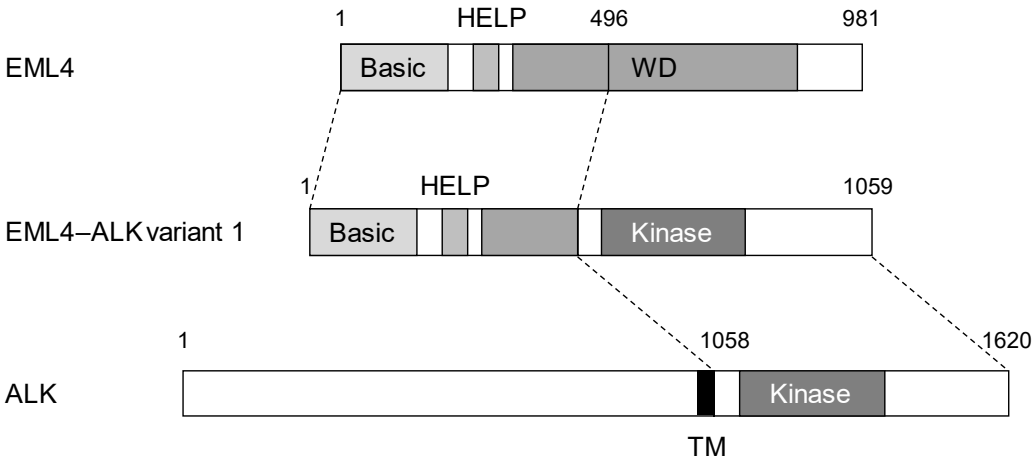

Figure 1. EML4–ALK fusion protein (minor modification of a schematic from reference [10]). Basic: basic region; HELP: HELP domain; WD: WD repeat; Kinase: tyrosine kinase domain; TM: transmembrane domain.

Since identification of the *EML4–ALK* fusion oncogene, research on ALK inhibitors has accelerated. Among the inhibitors reported, five tyrosine kinase inhibitors have been approved by the U.S. Food and Drug Administration (FDA) to date: crizotinib, discovered by Pfizer, was approved in 2011 [15]; ceritinib, discovered by Novartis Pharmaceuticals, was approved in 2014 [16, 17]; alectinib, discovered by Chugai Pharmaceutical, was approved in 2015 [18, 19]; brigatinib, discovered by ARIAD Pharmaceuticals, was approved in 2017 [20]; and lorlatinib, discovered by Pfizer, was approved in 2018 [21, 22]. The structures of these

approved inhibitors are shown in Figure 2 [23, 24]. Therefore, EML4–ALK is currently considered a valid therapeutic target for the treatment of EML4–ALK-positive NSCLC.

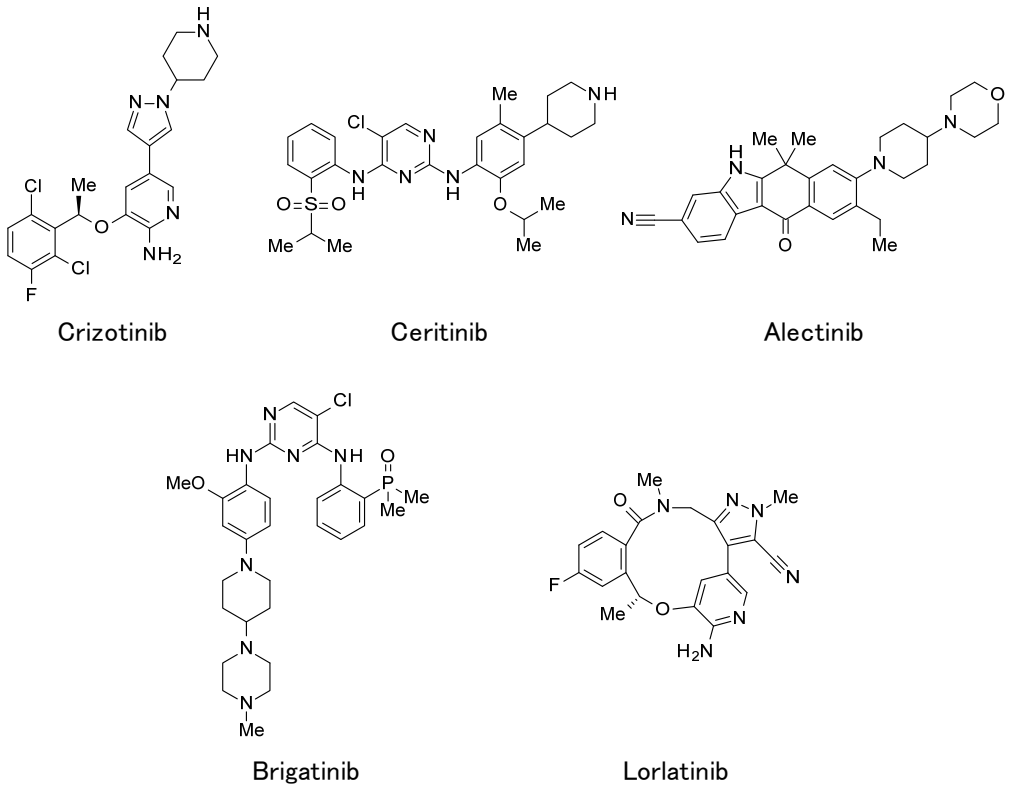

Figure 2. Structures of ALK inhibitors approved by the U.S. FDA.

This study aims to identify novel EML4–ALK inhibitors for the treatment of EML4–ALK-positive NSCLC. In Chapter 1, I describe the synthesis and biological evaluation of 1,3,5-triazine derivatives. I also discuss the detailed SAR studies conducted on each structural component of 1,3,5-triazine derivative compounds using computational modeling. In Chapter 2, I describe the synthesis and biological evaluation of pyrazine-2-carboxamide derivatives. I

also discuss the detailed SAR studies conducted on each structural component of pyrazine-2-carboxamide derivative compounds using computational modeling. Finally, I discuss the prospects of compounds found through this research in the conclusion part.

Chapter 1: Synthesis and structure–activity relationships of 1,3,5-triazine derivatives

1. Introduction

This research began with the aim of identifying novel EML4–ALK inhibitors. At that time, several compounds with inhibitory activity against ALK had been reported, such as NVP-TAE684 (Figure 3) [25]. In the course of exploring novel EML4–ALK inhibitors, 1,3,5-triazine derivatives were identified (Figure 3). Structural optimization of each component of these 1,3,5-triazine derivatives led to the identification of compound **12a** [26, 27]. Here, I describe the synthesis and biological evaluation of 1,3,5-triazine derivatives [28], along with studies on their SAR using computational modeling.

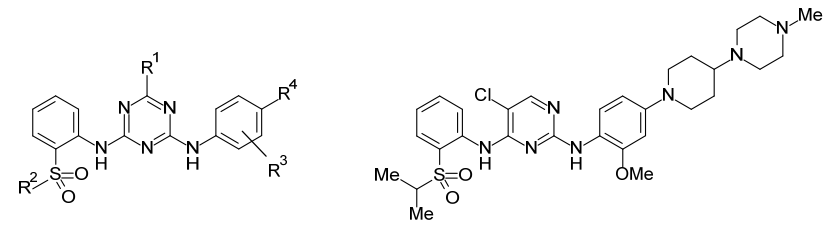

Figure 3. Structures of the 1,3,5-triazine substructure and NVP-TAE684.

2. Results and discussion

2.1 Chemistry

The synthesis of compounds **3a**–**e** is shown in Scheme 1. Compounds **3a**–**e** were synthesized by reacting **1a**–**c, 1d** [29], and **1e** [30] with 4-piperidone monohydrate monohydrochloride, followed by reductive amination with 1-methylpiperazine and sodium triacetoxyborohydride, and hydrogenation of the nitro groups with catalytic palladium on carbon.

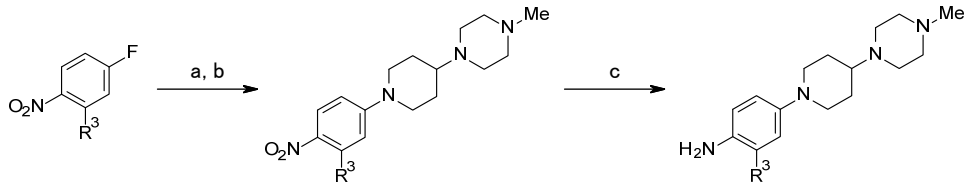

1a : R^3 = MeO
1b : R^3 = H
1c : R^3 = Me
1d : R^3 = EtO
1e : R^3 = *i*-PrO

2a : R^3 = MeO (56%)
2b : R^3 = H (14%)
2c : R^3 = Me (20%)
2d : R^3 = EtO (55%)
2e : R^3 = *i*-PrO (43%)

3a : R^3 = MeO (99%)
3b : R^3 = H (87%)
3c : R^3 = Me
3d : R^3 = EtO
3e : R^3 = *i*-PrO

Scheme 1. Synthesis of compounds **3a**–**e**.

Reagents and conditions: (a) 4-piperidone monohydrate monohydrochloride, K_2CO_3, DMF, 70 °C or 80 °C; (b) 1-methylpiperazine, $NaBH(OAc)_3$, DCM or DCE, rt; (c) H_2, 10% Pd/C, EtOH or EtOH/THF, rt.

The synthesis of compounds **6** and **8** is shown in Scheme 2 and Scheme 3, respectively. Compounds **6** and **8** were prepared by introducing commercially available corresponding amines into **4** and **1a**, followed by hydrogenation of the nitro groups with catalytic palladium on carbon.

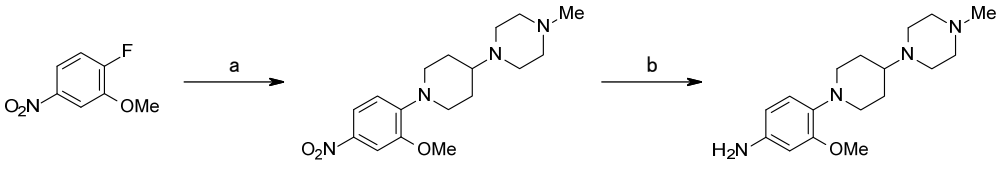

4 **5** **6**

Scheme 2. Synthesis of compound **6**.

Reagents and conditions: (a) 1-methyl-4-(piperidin-4-yl)piperazine, K_2CO_3, DMF, 80 °C, 95%; (b) H_2, 10% Pd/C, EtOH/THF, rt, 94%.

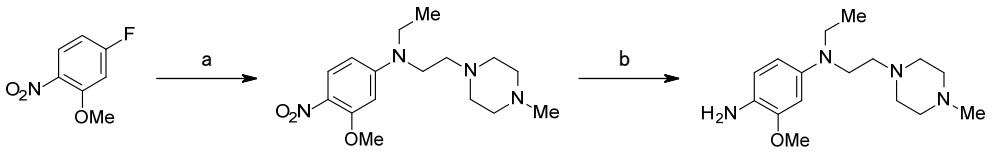

1a **7** **8**

Scheme 3. Synthesis of compound **8**.

Reagents and conditions: (a) *N*-ethyl-2-(4-methylpiperazin-1-yl)ethanamine, K_2CO_3, DMF, 80 °C, 43%; (b) H_2, 10% Pd/C, EtOH, rt.

The synthesis of compounds **12a**–**l** is shown in Scheme 4. Compounds **12a**–**l** were synthesized by reacting corresponding 1,3,5-triazine derivatives **9a, 9b**, and **9c** [31] with compounds **10a**–**c** [32] to yield 4-chloro-1,3,5-triazine derivatives **11a**–**e**, followed by the introduction of corresponding aniline derivatives using methanesulfonic acid in ethanol.

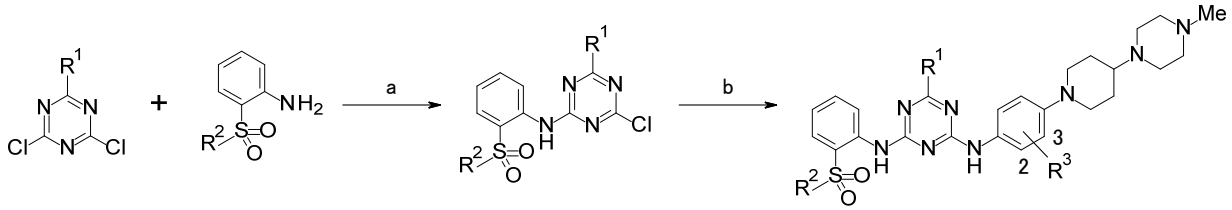

9a : R^1 = H
9b : R^1 = MeO
9c : R^1 = Me

10a : R^2 = *i*-Pr
10b : R^2 = Me
10c : R^2 = Et

11a : R^1 = H, R^2 = *i*-Pr (36%)
11b : R^1 = MeO, R^2 = *i*-Pr (29%)
11c : R^1 = Me, R^2 = *i*-Pr (18%)
11d : R^1 = H, R^2 = Me (52%)
11e : R^1 = H, R^2 = Et (47%)

12a : R^1 = H, R^2 = *i*-Pr, R^3 = 2-MeO (57%)
12b : R^1 = MeO, R^2 = *i*-Pr, R^3 = 2-MeO (50%)
12c : R^1 = Me, R^2 = *i*-Pr, R^3 = 2-MeO (19%)
12d : R^1 = H, R^2 = Me, R^3 = 2-MeO (31%)
12e : R^1 = H, R^2 = Et, R^3 = 2-MeO (18%)
12f : R^1 = H, R^2 = *i*-Pr, R^3 = 3-MeO (56%)
12g : R^1 = H, R^2 = *i*-Pr, R^3 = H (38%)
12h : R^1 = H, R^2 = *i*-Pr, R^3 = 2-Me (13%)*
12i : R^1 = H, R^2 = *i*-Pr, R^3 = 2-EtO (11%)*
12j : R^1 = H, R^2 = *i*-Pr, R^3 = 2-*i*-PrO (9%)*

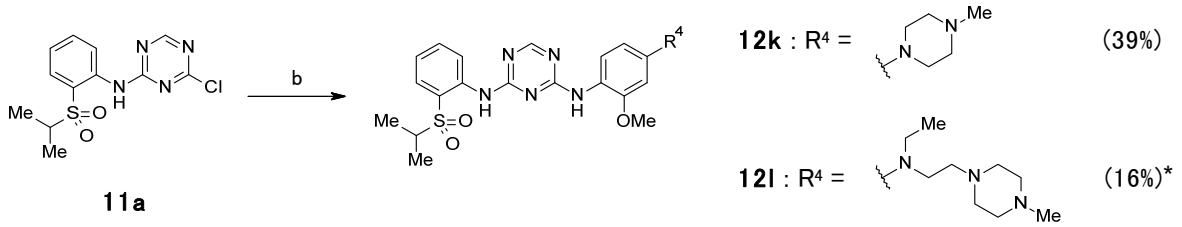

11a

12k : R^4 = (39%)

12l : R^4 = (16%)*

Scheme 4. Synthesis of compounds **12a**–**l**.

Reagents and conditions: (a) DIPEA, THF, rt or 70 °C; (b) **3a**–**e**, **6**, 2-methoxy-4-(4-methylpiperazin-1-yl)aniline [33], or **8**, MsOH, EtOH, 80 °C or 100 °C.

* 2-step yield from **2c**–**e** and **7**, respectively.

The synthesis of compound **18** is shown in Scheme 5. Compound **14** was prepared by reacting commercially available **13** with 2-bromopropane using a sodium hydroxymethanesulfinate-promoted one-pot reaction [34]. Oxidation of **14** with *m*-chloroperoxybenzoic acid, followed by reduction of the nitro group using iron powder in acetic acid produced compound **16**. Compound **16** was reacted with **9a** to obtain **17**, which was converted to **18** by introducing compound **3a**.

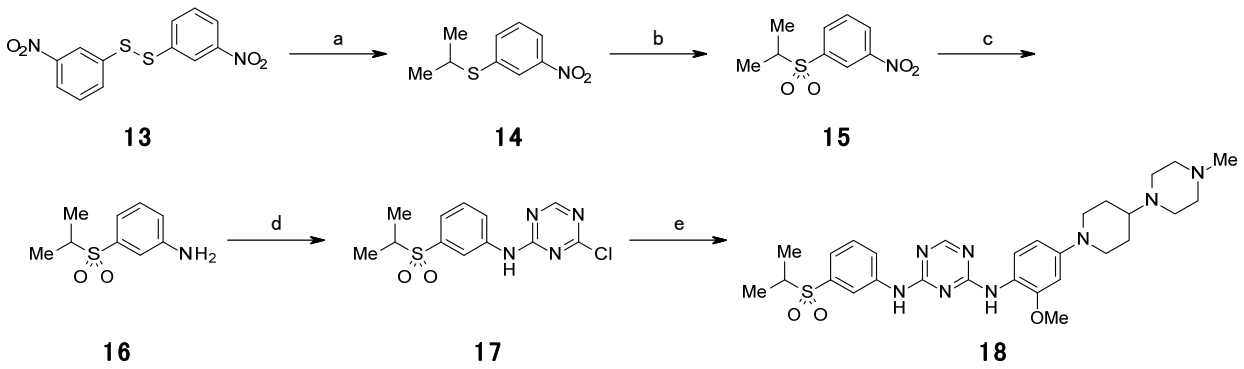

Scheme 5. Synthesis of compound **18**.

Reagents and conditions: (a) 2-bromopropane, sodium hydroxymethanesulfinate, K_2CO_3, DMF/H_2O, rt, 77%; (b) mCPBA, $CHCl_3$, rt to 50 °C, 99%; (c) Fe, AcOH, 80 °C, 63%; (d) **9a**, DIPEA, THF, 0 °C, 92%; (e) **3a**, MsOH, EtOH, 100 °C, 36%.

The synthesis of compound **23** is shown in Scheme 6. Compound **1a** was reacted with commercially available 1,4-dioxa-8-azaspiro[4.5]decane to give compound **19**, which was then hydrogenated to give compound **20**. The introduction of **20** into compound **11a** was performed using *N*,*N*-diisopropylethylamine in 1-methyl-2-pyrrolidone under microwave conditions at 120 °C to give compound **21**. After acidic hydrolysis of **21**, compound **22** was reacted with morpholine under reductive amination conditions, and subsequently treated with 4 M HCl in ethyl acetate to obtain compound **23** as a trihydrochloride salt.

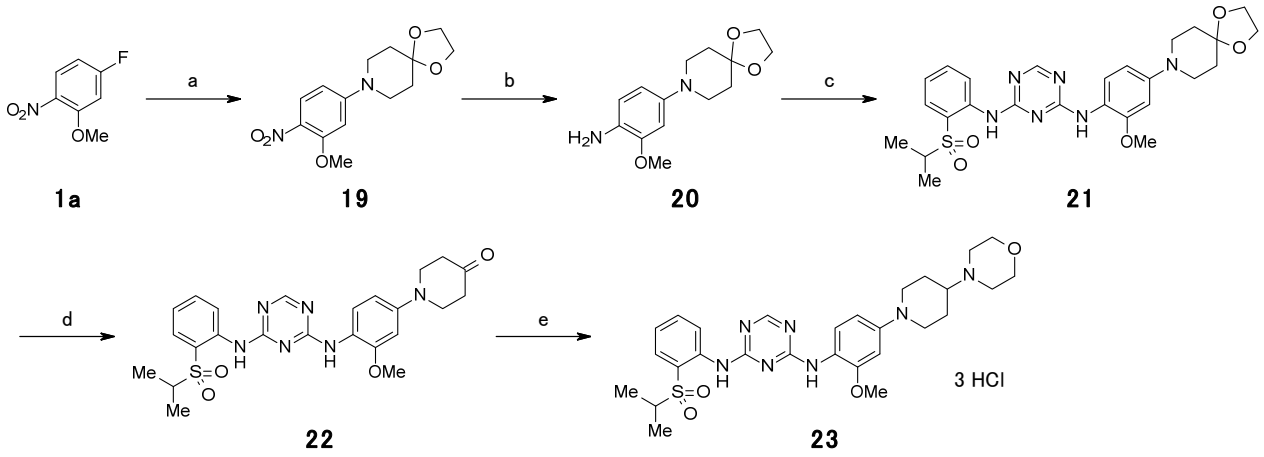

Scheme 6. Synthesis of compound **23**.

Reagents and conditions: (a) 1,4-dioxa-8-azaspiro[4.5]decane, K_2CO_3, DMF, 70 °C, 92%; (b) H_2, 10% Pd/C, EtOH/THF, rt, 82%; (c) **11a**, DIPEA, NMP, microwave, 120 °C, 94%; (d) 4 M HCl aq., 1,4-dioxane, 80 °C, 71%; (e) morpholine, $NaBH(OAc)_3$, DCM, rt, then 4 M HCl/EtOAc, THF, rt, 49%.

The synthesis of compound **27** is shown in Scheme 7. Compound **25** was synthesized by reacting **24** [35] with **11a** using *N*,*N*-diisopropylethylamine in 1-methyl-2-pyrrolidone under microwave conditions at 120 °C. After removal of the *tert*-butoxycarbonyl group of **25**, compound **26** was reacted with 1-methylpiperidin-4-one under reductive amination conditions to obtain compound **27**.

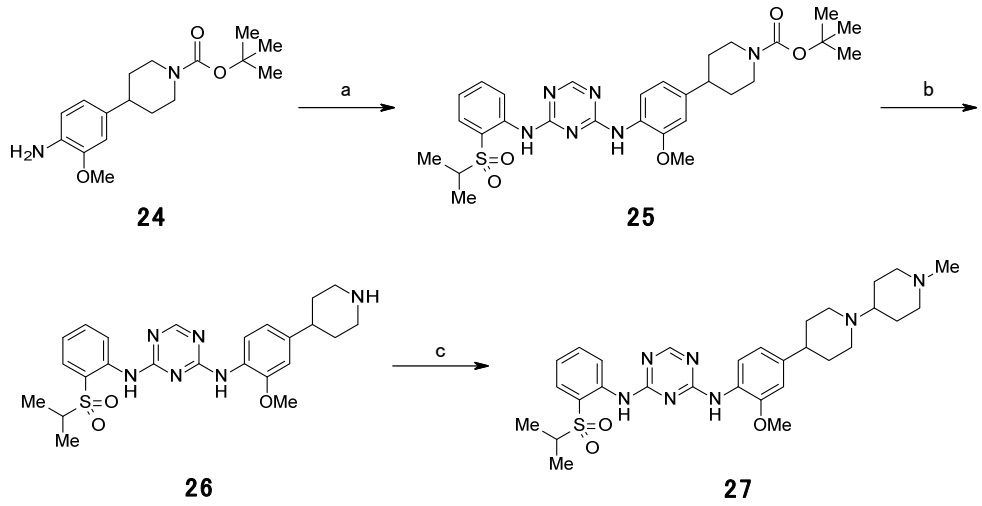

Scheme 7. Synthesis of compound **27**.

Reagents and conditions: (a) **11a**, DIPEA, NMP, microwave, 120 °C, 74%; (b) 4 M HCl/EtOAc, EtOAc/MeOH, rt, quantitative; (c) 1-methylpiperidin-4-one, $NaBH(OAc)_3$, DCM, rt, 39%.

2.2 Biological evaluation

The synthesized compounds were evaluated using the *in vitro* EML4–ALK inhibitory assay and cell growth assay in Ba/F3 cells expressing EML4–ALK. The SARs of R^1, R^2, R^3, and R^4 components are shown in Tables 1–4, respectively.

Table 1 shows the substituent effects at the 1,3,5-triazine ring. Introduction of a methoxy group (**12b**) and methyl group (**12c**) to the 1,3,5-triazine ring of **12a** led to a reduction in inhibitory activity against EML4–ALK compared to that of **12a** with IC_{50} values of 73 nM and 360 nM, respectively. The docking model of **12a** with ALK indicated the formation of two hydrogen bonds in the hinge region: (i) between one of the nitrogen atoms of the 1,3,5-triazine moiety and the NH hydrogen atom of Met1199, and (ii) between the hydrogen atom on the 1,3,5-triazine ring and the carbonyl oxygen atom of Glu1197 (Figure 4). Therefore, the decrease in inhibitory activity of **12b** and **12c** compared to that of **12a** may be attributed to the reduction in interaction between these compounds and the hinge region in ALK.

Table 1. Structure-activity relationship of compounds **12a**–**c**.

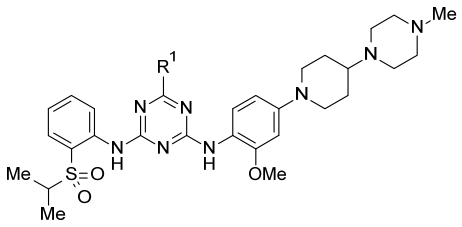

Compound	R^1	EML4–ALK IC_{50} (nM)	Ba/F3 IC_{50} (nM)
12a	H	17	42
12b	MeO	73	304
12c	Me	360	NT[a]

[a] Not tested.

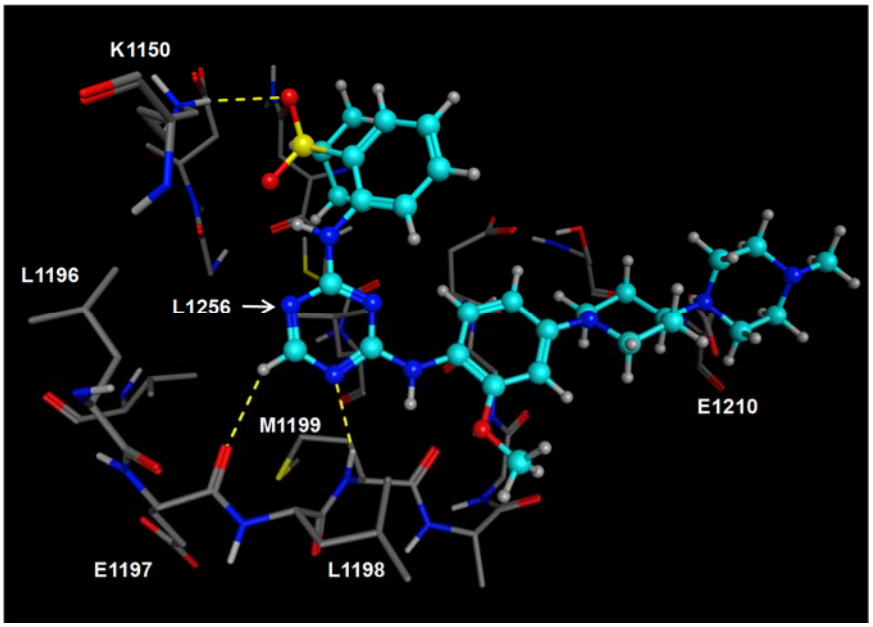

Figure 4. Docking mode of **12a** with ALK [27].

Compound **12a** and ALK are represented as a ball-and-stick and stick model, respectively. All of the atoms are colored by element (white: hydrogen, cyan: carbon of **12a**, gray: carbon of ALK, blue: nitrogen, red: oxygen, yellow: sulfur). The yellow dotted lines indicate the hydrogen bonds formed between **12a** and ALK. For clarity, the non-polar hydrogen atoms of the protein have been omitted, and all atoms of ALK closer than the front of the gatekeeper residue are hidden.

Table 2 shows the SAR of the sulfonyl moiety of compound **12a**. Substitution of the 2-isopropylsulfonyl group of **12a** with a 3-isopropylsulfonyl group (**18**) resulted in a loss of inhibitory activity against EML4–ALK, possibly due to the steric hindrance between compound **18** and amino acid residues, including Gly1125 and Ala1126 (Figure 5). The methylsulfonyl derivative **12d** exhibited a decrease in inhibitory activity against EML4–ALK (**12d**: IC_{50} = 530 nM), while the ethylsulfonyl derivative **12e** retained inhibitory activity against EML4–ALK (**12e**: IC_{50} = 21 nM). The docking model suggested that the 2-isopropylsulfonyl moiety of compound **12a** plays two important roles with respect to inhibitory activity against EML4–ALK: (i) the oxygen atom of the sulfone interacts with Lys1150, and (ii) one of the two methyl groups of the isopropyl moiety extends into the hydrophobic pocket formed by Leu1256 and forms a hydrophobic interaction (Figure 5). Therefore, the decrease in inhibitory activity observed for compound **12d** compared to that of **12a** may be attributed to the loss of hydrophobic interaction between compound **12d** and the hydrophobic pocket. In contrast, compound **12e** retained inhibitory activity, possibly because the ethyl group of compound **12e** can occupy the hydrophobic pocket.

Table 2. Structure-activity relationship of compounds **12a**, **12d**, **12e**, and **18**.

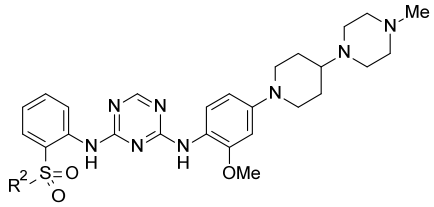

12a, **12d**, **12e**

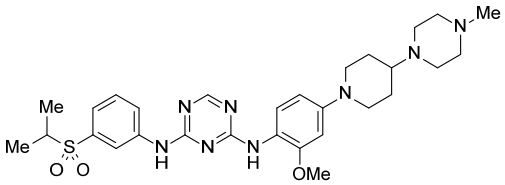

18

Compound	R^2	EML4–ALK IC_{50} (nM)	Ba/F3 IC_{50} (nM)
12a	*i*-Pr	17	42
12d	Me	530	NT[a]
12e	Et	21	146
18	—	> 1000	NT[a]

[a] Not tested.

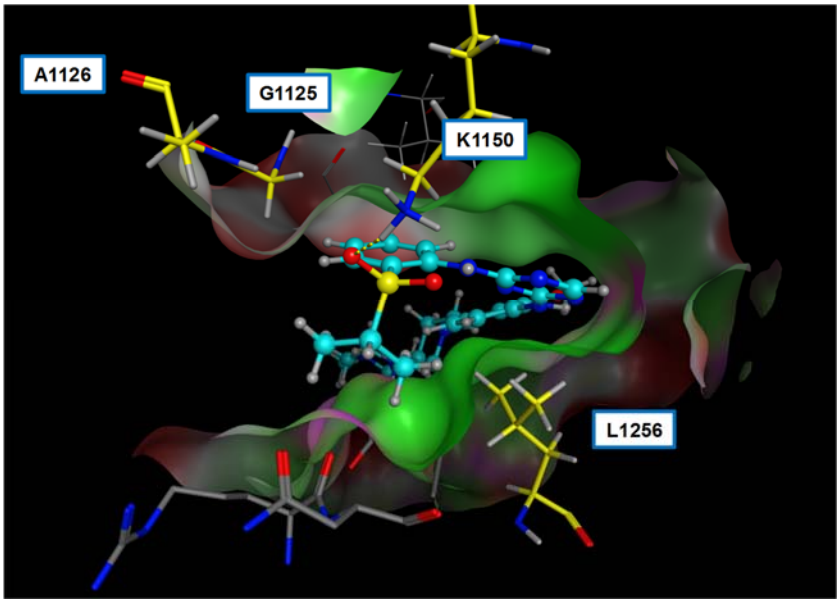

Figure 5. Docking mode of **12a** with ALK [27].

Compound **12a** and ALK are represented as a ball-and-stick and stick model, respectively. The protein surface is colored according to the characteristics of the pocket (green: hydrophobic, magenta: polar, red: solvent exposed). The carbon atoms of A1126, G1125, K1150, and L1256 are highlighted in yellow. The other colors and visualization schemes are the same as those in Figure 4.

Table 3 shows the substituent effects at the methoxy component of **12a**. Replacement of the 2-methoxy group (**12a**) with a 3-methoxy group (**12f**) resulted in a three-fold reduction in inhibitory activity against EML4–ALK compared to that of **12a**. The unsubstituted compound **12g** showed a 19-fold decrease in inhibitory activity against EML4–ALK compared to that of **12a**. Substitution of the methoxy group of compound **12a** with a methyl group (**12h**) also reduced the inhibitory activity against EML4–ALK. These results indicate that the oxygen atom in the 2-methoxy group of compound **12a** is important for the inhibitory activity of the compound, possibly because the methoxy group of **12a** forms a dipole–dipole interaction with the NH at the 2-position of the 1,3,5-triazine ring that stabilizes the desirable conformation (Figure 4). Replacement of the methoxy group of **12a** with an ethoxy group (**12i**) and an isopropoxy group (**12j**) also resulted in a decrease in inhibitory activity against EML4–ALK compared to that of **12a** with IC_{50} values of 93 nM and 210 nM, respectively. These results may be explained by the relatively narrow space between the 2-methoxy group of **12a** and ALK suggested by the docking model (Figure 4).

Table 3. Structure-activity relationship of compounds **12a** and **12f**–**j**.

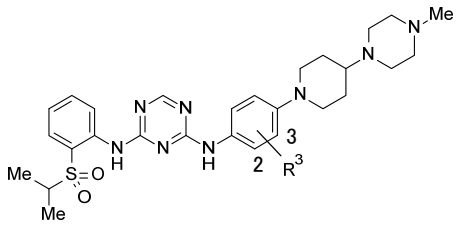

Compound	R^3	EML4–ALK IC_{50} (nM)	Ba/F3 IC_{50} (nM)
12a	2-MeO	17	42
12f	3-MeO	56	107
12g	H	330	NT[a]
12h	2-Me	340	NT[a]
12i	2-EtO	93	197
12j	2-*i*-PrO	210	NT[a]

[a] Not tested.

Table 4 shows the SAR of the amine moiety in **12a**. According to the docking model, this group extends into the solvent-exposed region located outside the ATP-binding pocket and adjacent to Glu1210 (Figure 4). Compounds **12k** and **23** retained inhibitory activity against EML4–ALK with IC_{50} values of 29 nM and 28 nM, respectively. Compound **27** showed potent inhibitory activity against EML4–ALK with an IC_{50} value of 7.9 nM, while compound **12l** showed a five-fold reduction in inhibitory activity against EML4–ALK. Among these compounds, compound **12a** exhibited the most promising *in vitro* profile based on the results of both the EML4–ALK inhibitory assay and cell growth assay in Ba/F3 cells. Therefore, compound **12a** was selected for examination of antitumor activity (Figure 6).

Table 4. Structure-activity relationship of compounds **12a**, **12k**, **12l**, **23**, and **27**.

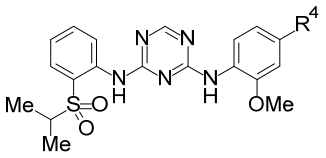

Compound	R^4	EML4–ALK IC_{50} (nM)	Ba/F3 IC_{50} (nM)
12a	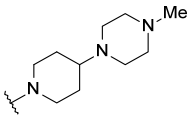	17	42
12k	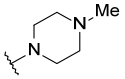	29	67
23[a]	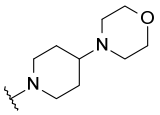	28	208
27	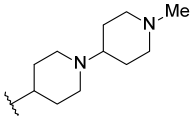	7.9	61
12l	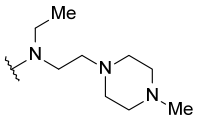	81	ND[b]

[a] 3HCl salt.

[b] Not determined.

The antitumor activity of **12a** was evaluated in mice xenografted with NCI-H2228, human NSCLC tumor cells that endogenously express EML4–ALK (Figure 7). Once-daily oral administration of **12a** for 14 days demonstrated tumor growth inhibition at doses of 0.3 mg/kg (4% inhibition) and 1 mg/kg (69% inhibition), and tumor regression at doses of 3 mg/kg (4% regression), 10 mg/kg (45% regression), and 30 mg/kg (78% regression) in a dose-dependent manner. Body weight was not affected by **12a** at the doses used in this experiment [26].

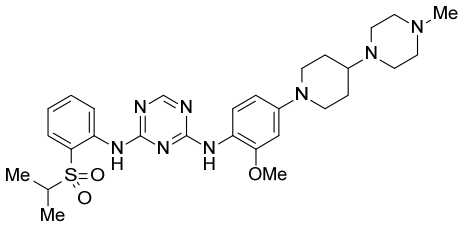

12a (ASP3026)

Figure 6. Structure of **12a** (ASP3026).

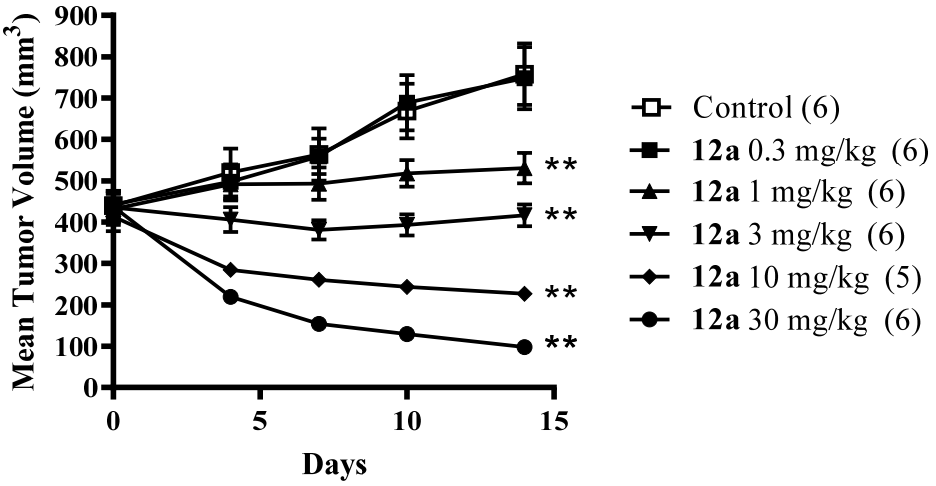

Figure 7. Antitumor activity of **12a** [26, 27].

Mice subcutaneously xenografted with NCI-H2228 cells were treated with once-daily oral administration of **12a** at the indicated doses for 14 days. Tumor volume was measured to assess antitumor activity. Each point represents the mean ± SEM, and the number of animals used is shown in parentheses. The values obtained on day 14 were statistically analyzed and compared. **, $P < 0.01$ compared with the value of the control group on day 14 (Dunnett's multiple comparison test).

3. Experimental section

Chemistry

^{1}H NMR spectra were recorded on JEOL AL400 or Varian 400-MR, and chemical shifts were expressed in δ (ppm) values with tetramethylsilane as an internal reference (s = singlet, d = doublet, t = triplet, q = quartet, m = multiplet, dd = doublet of doublets, and br = broad peak). Mass spectra (MS) were recorded on Thermo Electron LCQ Advantage, Waters UPLC/ZQ, Waters UPLC/SQD LC/MS system, JEOL GCmate Ⅱ, Thermo Electron TRACE DSQ or Waters Micromass LCT Premier Mass Spectrometer. Elemental analyses were performed with Yanaco MT-6 (C, H, N) and DIONEX DX-500 (S, halogen) instruments, and results were within ±0.3% of theoretical values.

1-[1-(3-Methoxy-4-nitrophenyl)piperidin-4-yl]-4-methylpiperazine (**2a**)

To a mixture of 4-fluoro-2-methoxy-1-nitrobenzene (**1a**, 3.00 g, 17.5 mmol) and K_2CO_3 (6.10 g, 44.1 mmol) in DMF (30 mL) was added 4-piperidone monohydrate monohydrochloride (3.20 g, 20.8 mmol). The reaction mixture was stirred at 70 °C overnight. Water was added to the mixture, and the resulting slurry was extracted with EtOAc. The organic layer was washed with water and brine, dried over Na_2SO_4, and concentrated *in vacuo*. The residue was washed with Et_2O to give an ocher solid (3.85 g).

To this product were added 1,2-dichloroethane (40 mL) and 1-methylpiperazine (2 mL, 18.2 mmol). After the mixture was stirred for 30 min, sodium triacetoxyborohydride (3.90 g, 18.4 mmol) was added to the mixture, and the reaction mixture was stirred at room temperature

overnight. Saturated aqueous $NaHCO_3$ solution was added to the mixture, and the resulting slurry was extracted with $CHCl_3$. The organic layer was dried over Na_2SO_4, and concentrated *in vacuo*. The residue was purified by silica gel column chromatography ($CHCl_3$/MeOH/28% aqueous NH_3 = 30:1:0.1 to 15:1:0.1). The resulting solid was washed with *n*-hexane to give **2a** (3.30 g, 56%) as a yellow solid. ^{1}H NMR ($CDCl_3$): δ 1.52–1.69 (2H, m), 1.90–2.03 (2H, m), 2.20–2.80 (9H, m), 2.31 (3H, s), 2.90–3.03 (2H, m), 3.89–4.01 (2H, m), 3.95 (3H, s), 6.31 (1H, d, *J* = 2.0 Hz), 6.42 (1H, dd, *J* = 2.0, 9.2 Hz), 7.96–8.03 (1H, m); MS (ESI) *m/z* $[M+H]^+$ 335.

1-Methyl-4-[1-(4-nitrophenyl)piperidin-4-yl]piperazine (**2b**)

Compound **2b** was prepared with a yield of 14% from 1-fluoro-4-nitrobenzene (**1b**) using a procedure similar to that described for **2a**. ^{1}H NMR ($CDCl_3$): δ 1.52–1.73 (2H, m), 1.88–2.02 (2H, m), 2.18–2.76 (9H, m), 2.29 (3H, s), 2.89–3.05 (2H, m), 3.91–4.05 (2H, m), 6.75–6.85 (2H, m), 8.06–8.15 (2H, m); MS (ESI) *m/z* $[M+H]^+$ 305.

1-Methyl-4-[1-(3-methyl-4-nitrophenyl)piperidin-4-yl]piperazine (**2c**)

Compound **2c** was prepared with a yield of 20% from 4-fluoro-2-methyl-1-nitrobenzene (**1c**) using a procedure similar to that described for **2a**. ^{1}H NMR (DMSO-d_6): δ 1.32–1.47 (2H, m), 1.75–1.88 (2H, m), 2.12 (3H, s), 2.15–2.63 (8H, m), 2.55 (3H, s), 2.85–3.00 (2H, m), 3.36–3.44 (1H, m), 3.95–4.11 (2H, m), 6.81–6.93 (2H, m), 7.93–8.02 (1H, m); MS

(ESI) *m/z* $[M+H]^+$ 319.

1-[1-(3-Ethoxy-4-nitrophenyl)piperidin-4-yl]-4-methylpiperazine (**2d**)

Compound **2d** was prepared with a yield of 55% from 2-ethoxy-4-fluoro-1-nitrobenzene (**1d**) using a procedure similar to that described for **2a**. ^{1}H NMR ($CDCl_3$): δ 1.50 (3H, t, *J* = 7.0 Hz), 1.53–1.67 (2H, m), 1.88–2.01 (2H, m), 2.22–2.75 (9H, m), 2.29 (3H, s), 2.86–3.00 (2H, m), 3.84–3.98 (2H, m), 4.14 (2H, q, *J* = 6.9 Hz), 6.31 (1H, d, *J* = 2.8 Hz), 6.41 (1H, dd, *J* = 2.6, 9.4 Hz), 7.97 (1H, d, *J* = 9.2 Hz); MS (FAB) *m/z* $[M+H]^+$ 349.

1-Methyl-4-{1-[4-nitro-3-(propan-2-yloxy)phenyl]piperidin-4-yl}piperazine (**2e**)

Compound **2e** was prepared with a yield of 43% from 4-fluoro-1-nitro-2-(propan-2-yloxy)benzene (**1e**) using a procedure similar to that described for **2a**. ^{1}H NMR ($CDCl_3$): δ 1.41 (6H, d, *J* = 6.4 Hz), 1.52–1.68 (2H, m), 1.88–2.01 (2H, m), 2.19–2.76 (9H, m), 2.29 (3H, s), 2.87–2.99 (2H, m), 3.82–3.95 (2H, m), 4.53–4.67 (1H, m), 6.35 (1H, d, *J* = 2.4 Hz), 6.42 (1H, dd, *J* = 2.8, 9.6 Hz), 7.94 (1H, d, *J* = 9.6 Hz); MS (ESI) *m/z* $[M+H]^+$ 363.

2-Methoxy-4-[4-(4-methylpiperazin-1-yl)piperidin-1-yl]aniline (**3a**)

To a mixture of 1-[1-(3-methoxy-4-nitrophenyl)piperidin-4-yl]-4-methylpiperazine (**2a**, 2.18 g, 6.52 mmol) in EtOH (50 mL) was added 10% palladium on carbon (wet, contains

53% water; 600 mg). The reaction mixture was stirred at room temperature for 8 h under 1 atm hydrogen atmosphere. The insoluble material was removed by filtration through Celite, and the filtrate was concentrated *in vacuo* to give **3a** (1.96 g, 99%) as a pale purple solid. ^{1}H NMR ($CDCl_3$): δ 1.62–1.80 (2H, m), 1.86–1.98 (2H, m), 2.22–2.84 (11H, m), 2.31 (3H, s), 3.23–3.74 (4H, m), 3.83 (3H, s), 6.42 (1H, dd, J = 2.4, 8.0 Hz), 6.52 (1H, d, J = 2.4 Hz), 6.63 (1H, d, J = 8.4 Hz); MS (EI) *m/z* $[M]^+$ 304.

4-[4-(4-Methylpiperazin-1-yl)piperidin-1-yl]aniline (**3b**)

Compound **3b** was prepared with a yield of 87% from **2b** using a procedure similar to that described for **3a**. ^{1}H NMR (DMSO-d_6): δ 1.39–1.56 (2H, m), 1.72–1.86 (2H, m), 2.07–2.61 (11H, m), 2.13 (3H, s), 3.25–3.46 (2H, m), 4.53 (2H, s), 6.43–6.51 (2H, m), 6.63–6.70 (2H, m); MS (ESI) *m/z* $[M+H]^+$ 275.

2-Methyl-4-[4-(4-methylpiperazin-1-yl)piperidin-1-yl]aniline (**3c**)

Compound **3c** was prepared from **2c** using a procedure similar to that described for **3a**. MS (ESI) *m/z* $[M+H]^+$ 289.

2-Ethoxy-4-[4-(4-methylpiperazin-1-yl)piperidin-1-yl]aniline (**3d**)

Compound **3d** was prepared from **2d** using a procedure similar to that described for

3a. MS (ESI) *m/z* $[M+H]^+$ 319.

4-[4-(4-Methylpiperazin-1-yl)piperidin-1-yl]-2-(propan-2-yloxy)aniline (**3e**)

Compound **3e** was prepared from **2e** using a procedure similar to that described for **3a**. MS (ESI) *m/z* $[M+H]^+$ 333.

1-[1-(2-Methoxy-4-nitrophenyl)piperidin-4-yl]-4-methylpiperazine (**5**)

To a solution of 1-fluoro-2-methoxy-4-nitrobenzene (**4**, 4.74 g, 27.7 mmol) in DMF (47 mL) were added 1-methyl-4-(piperidin-4-yl)piperazine (5.33 g, 29.1 mmol) and K_2CO_3 (4.59 g, 33.2 mmol). The reaction mixture was stirred at 80 °C for 15 h. Water was added to this reaction mixture under cooling in an ice bath, and the resulting precipitate was filtered and washed with water to give **5** (8.79 g, 95%) as a yellow solid. ^{1}H NMR (DMSO-d_6): δ 1.44–1.60 (2H, m), 1.77–1.89 (2H, m), 2.06–2.61 (9H, m), 2.14 (3H, s), 2.65–2.80 (2H, m), 3.63–3.76 (2H, m), 3.90 (3H, s), 7.00 (1H, d, J = 8.8 Hz), 7.67 (1H, d, J = 2.4 Hz), 7.82 (1H, dd, J = 2.4, 8.8 Hz); MS (ESI) *m/z* $[M+H]^+$ 335.

3-Methoxy-4-[4-(4-methylpiperazin-1-yl)piperidin-1-yl]aniline (**6**)

Compound **6** was prepared with a yield of 94% from **5** using a procedure similar to that described for **3a**. ^{1}H NMR ($CDCl_3$): δ 1.72–1.94 (4H, m), 2.29 (3H, s), 2.32–2.77 (11H,

m), 3.32–3.60 (4H, m), 3.81 (3H, s), 6.19–6.29 (2H, m), 6.77 (1H, d, J = 8.4 Hz); MS (ESI) *m/z* $[M+H]^+$ 305.

_N_-Ethyl-3-methoxy-_N_-[2-(4-methylpiperazin-1-yl)ethyl]-4-nitroaniline (**7**)

A mixture of 4-fluoro-2-methoxy-1-nitrobenzene (**1a**, 900 mg, 5.26 mmol), *N*-ethyl-2-(4-methylpiperazin-1-yl)ethanamine (901 mg, 5.26 mmol) and K_2CO_3 (727 mg, 5.26 mmol) in DMF (10 mL) was stirred at 80 °C for 6 h. The solvent was concentrated, then water was added to the residue. The slurry was extracted with EtOAc, and the organic layer was washed with brine, dried over anhydrous $MgSO_4$, and concentrated *in vacuo*. The residue was purified by silica gel column chromatography ($CHCl_3$ to $CHCl_3$/MeOH/28% aqueous NH_3 = 10/1/0.1) to give **7** (730 mg, 43%). ^{1}H NMR (DMSO-d_6): δ 1.14 (3H, t, J = 6.6 Hz), 2.14 (3H, s), 2.17–2.60 (10H, m), 3.42–3.59 (4H, m), 3.90 (3H, s), 6.19–6.24 (1H, m), 6.31–6.38 (1H, m), 7.86–7.93 (1H, m); MS (ESI) *m/z* $[M+H]^+$ 323.

N^4-Ethyl-2-methoxy-N^4-[2-(4-methylpiperazin-1-yl)ethyl]benzene-1,4-diamine (**8**)

Compound **8** was prepared from **7** using a procedure similar to that described for **3a** and directly used in the next reaction. MS (ESI) *m/z* $[M+H]^+$ 293.

4-Chloro-_N_-[2-(propane-2-sulfonyl)phenyl]-1,3,5-triazin-2-amine (**11a**)

To a mixture of 2,4-dichloro-1,3,5-triazine (**9a**, 460 mg, 3.07 mmol) and THF (5 mL) was added a mixture of 2-(propane-2-sulfonyl)aniline (**10a**, 600 mg, 3.01 mmol) and DIPEA (0.58 mL, 3.33 mmol) in THF (10 mL). After the reaction mixture was stirred at room temperature for three days, water (60 mL) and saturated aqueous $NaHCO_3$ solution were added. The resulting slurry was extracted with EtOAc, and the organic layer was washed with water and brine, dried over Na_2SO_4, and concentrated *in vacuo*. The residue was purified by silica gel column chromatography ($CHCl_3$) to give **11a** (340 mg, 36%) as a white solid. ^{1}H NMR ($CDCl_3$): δ 1.32 (6H, d, J = 7.2 Hz), 3.15–3.30 (1H, m), 7.30–7.38 (1H, m), 7.67–7.76 (1H, m), 7.92 (1H, dd, J = 1.5, 7.8 Hz), 8.47–8.53 (1H, m), 8.61 (1H, s), 9.66–10.13 (1H, br); MS (ESI) *m/z* $[M+H]^+$ 313.

4-Chloro-6-methoxy-*N*-[2-(propane-2-sulfonyl)phenyl]-1,3,5-triazin-2-amine (**11b**)

To a mixture of 2,4-dichloro-6-methoxy-1,3,5-triazine (**9b**, 370 mg, 2.06 mmol) and THF (10 mL) was added a mixture of 2-(propane-2-sulfonyl)aniline (**10a**, 400 mg, 2.01 mmol) and DIPEA (0.72 mL, 4.13 mmol) in THF (5 mL). After the reaction mixture was stirred at room temperature overnight and at 70 °C for 7 h, water (60 mL) was added under ice-cooling. The resulting solid was purified by silica gel column chromatography ($CHCl_3$) and washed with *n*-hexane to give **11b** (200 mg, 29%) as a white solid. ^{1}H NMR ($CDCl_3$): δ 1.31 (6H, d, J = 6.8 Hz), 3.13–3.28 (1H, m), 4.06 (3H, s), 7.19–7.38 (1H, m), 7.60–7.74 (1H, m), 7.90 (1H, dd, J =

1.6, 7.6 Hz), 8.47 (1H, dd, *J* = 1.0, 8.2 Hz), 9.69 (1H, s); MS (ESI) *m/z* $[M+H]^+$ 343.

4-Chloro-6-methyl-*N*-[2-(propane-2-sulfonyl)phenyl]-1,3,5-triazin-2-amine (**11c**)

Compound **11c** was prepared with a yield of 18% from 2-(propane-2-sulfonyl)aniline (**10a**) and 2,4-dichloro-6-methyl-1,3,5-triazine (**9c**) using a procedure similar to that described for **11a**. ^{1}H NMR (DMSO-d_6): δ 1.14 (6H, d, *J* = 6.8 Hz), 2.40 (3H, s), 3.44–3.57 (1H, m), 7.47–7.60 (1H, m), 7.78–7.86 (1H, m), 7.91 (1H, dd, *J* = 1.6, 8.0 Hz), 7.99–8.10 (1H, m), 10.00 (1H, s); MS (FAB) *m/z* $[M+H]^+$ 327.

4-Chloro-*N*-[2-(methanesulfonyl)phenyl]-1,3,5-triazin-2-amine (**11d**)

To a mixture of 2-(methanesulfonyl)aniline monohydrochloride (**10b**, 600 mg, 2.89 mmol) and THF (10 mL) were added DIPEA (1.2 mL, 6.89 mmol) and 2,4-dichloro-1,3,5-triazine (**9a**, 880 mg, 5.87 mmol) under ice-cooling. After the reaction mixture was stirred at room temperature overnight, saturated aqueous $NaHCO_3$ solution and water were added. The resulting slurry was extracted with EtOAc, and the organic layer was washed with water and brine, dried over Na_2SO_4, and concentrated *in vacuo*. The residue was purified by silica gel column chromatography (*n*-hexane/EtOAc = 3:1 to 2:1) and washed with Et_2O to give **11d** (430 mg, 52%) as a white solid. ^{1}H NMR ($CDCl_3$): δ 3.10 (3H, s), 7.31–7.41 (1H, m), 7.67–7.78 (1H, m), 7.97–8.07 (1H, m), 8.42–8.51 (1H, m), 8.63 (1H, s), 9.48–9.74 (1H, br); MS (FAB) *m/z*

$[M+H]^+$ 285.

4-Chloro-*N*-[2-(ethanesulfonyl)phenyl]-1,3,5-triazin-2-amine (**11e**)

Compound **11e** was prepared with a yield of 47% from 2-(ethanesulfonyl)aniline (**10c**) and 2,4-dichloro-1,3,5-triazine (**9a**) using a procedure similar to that described for **11d**. ^{1}H NMR ($CDCl_3$): δ 1.29 (3H, t, *J* = 7.4 Hz), 3.16 (2H, q, *J* = 7.5 Hz), 7.31–7.40 (1H, m), 7.67–7.78 (1H, m), 7.96 (1H, dd, *J* = 1.6, 8.0 Hz), 8.45–8.52 (1H, m), 8.62 (1H, s), 9.61–9.90 (1H, br); MS (ESI) *m/z* $[M+H]^+$ 299.

***N*-{2-Methoxy-4-[4-(4-methylpiperazin-1-yl)piperidin-1-yl]phenyl}-*N*'-[2-(propane-2-sulfonyl)phenyl]-1,3,5-triazine-2,4-diamine** (**12a**, ASP3026)

A mixture of **3a** (210 mg, 0.690 mmol) and MsOH (0.13 mL, 2.00 mmol) in EtOH (3mL) was stirred at room temperature for 15 min. To this mixture was added **11a** (170 mg, 0.543 mmol), and the reaction mixture was stirred at 100 °C for 2 h. After the mixture was cooled to room temperature, water and saturated aqueous $NaHCO_3$ solution were added. The resulting slurry was extracted with $CHCl_3$, and the organic layer was dried over Na_2SO_4, then concentrated *in vacuo*. The residue was purified by silica gel column chromatography ($CHCl_3$/MeOH/28% aqueous NH_3 = 50:1:0.1 to 30:1:0.1) to give **12a** (180 mg, 57%). ^{1}H NMR ($CDCl_3$): δ 1.31 (6H, d, *J* = 6.8 Hz), 1.62–1.79 (2H, m), 1.90–2.02 (2H, m), 2.23–2.81 (11H,

m), 2.30 (3H, s), 3.18–3.32 (1H, m), 3.63–3.75 (2H, m), 3.88 (3H, s), 6.45–6.62 (2H, m), 7.14–7.29 (1H, m), 7.43–7.71 (2H, m), 7.88 (1H, dd, *J* = 1.6, 8.0 Hz), 8.02–8.17 (1H, m), 8.27–8.61 (2H, m), 9.28 (1H, s); MS (ESI) *m/z* $[M+H]^+$ 581; HRMS (ESI) *m/z* Calcd for $C_{29}H_{41}N_8O_3S$ $[M+H]^+$: 581.3022, Found: 581.3022.

6-Methoxy-*N*-{2-methoxy-4-[4-(4-methylpiperazin-1-yl)piperidin-1-yl]phenyl}-*N*'-[2-(propane-2-sulfonyl)phenyl]-1,3,5-triazine-2,4-diamine (**12b**)

Compound **12b** was prepared with a yield of 50% from **3a** and **11b** using a procedure similar to that described for **12a**. ^{1}H NMR ($CDCl_3$): δ 1.30 (6H, d, *J* = 6.8 Hz), 1.50–1.79 (2H, m), 1.88–2.01 (2H, m), 2.25–2.81 (11H, m), 2.30 (3H, s), 3.19–3.32 (1H, m), 3.62–3.74 (2H, m), 3.89 (3H, s), 3.99 (3H, s), 6.44–6.60 (2H, m), 7.13–7.24 (1H, m), 7.47 (1H, s), 7.56–7.66 (1H, m), 7.87 (1H, dd, *J* = 1.6, 8.0 Hz), 8.08–8.27 (1H, br), 8.47–8.62 (1H, m), 9.20 (1H, s); MS (ESI) *m/z* $[M+H]^+$ 611; HRMS (ESI) *m/z* Calcd for $C_{30}H_{43}N_8O_4S$ $[M+H]^+$: 611.3128, Found: 611.3140.

***N*-{2-Methoxy-4-[4-(4-methylpiperazin-1-yl)piperidin-1-yl]phenyl}-6-methyl-*N*'-[2-(propane-2-sulfonyl)phenyl]-1,3,5-triazine-2,4-diamine** (**12c**)

Compound **12c** was prepared with a yield of 19% from **3a** and **11c** using a procedure similar to that described for **12a**. ^{1}H NMR ($CDCl_3$): δ 1.31 (6H, d, *J* = 6.8 Hz), 1.50–1.79 (2H,

m), 1.89–2.01 (2H, m), 2.22–2.79 (11H, m), 2.30 (3H, s), 2.41 (3H, s), 3.19–3.32 (1H, m), 3.61–3.74 (2H, m), 3.87 (3H, s), 6.45–6.58 (2H, m), 7.14–7.23 (1H, m), 7.35–7.55 (1H, m), 7.55–7.68 (1H, m), 7.87 (1H, dd, J = 1.6, 8.0 Hz), 8.04–8.30 (1H, br), 8.53–8.67 (1H, m), 9.23 (1H, s); MS (ESI) *m/z* $[M+H]^+$ 595; HRMS (ESI) *m/z* Calcd for $C_{30}H_{43}N_8O_3S$ $[M+H]^+$: 595.3179, Found: 595.3171.

_N_-[2-(Methanesulfonyl)phenyl]-_N_'-{2-methoxy-4-[4-(4-methylpiperazin-1-yl)piperidin-1-yl]phenyl}-1,3,5-triazine-2,4-diamine (12d)

Compound **12d** was prepared with a yield of 31% from **3a** and **11d** using a procedure similar to that described for **12a**. ^{1}H NMR ($CDCl_3$): δ 1.49–1.79 (2H, m), 1.88–2.01 (2H, m), 2.30 (3H, s), 2.32–2.83 (11H, m), 3.09 (3H, s), 3.62–3.75 (2H, m), 3.88 (3H, s), 6.44–6.61 (2H, m), 7.18–7.29 (1H, m), 7.49–7.71 (2H, m), 7.97 (1H, dd, J = 1.6, 8.0 Hz) 8.01–8.16 (1H, m), 8.28–8.56 (2H, m), 9.00 (1H, s); MS (ESI) *m/z* $[M+H]^+$ 553; HRMS (ESI) *m/z* Calcd for $C_{27}H_{37}N_8O_3S$ $[M+H]^+$: 553.2709, Found: 553.2701.

_N_-[2-(Ethanesulfonyl)phenyl]-_N_'-{2-methoxy-4-[4-(4-methylpiperazin-1-yl)piperidin-1-yl]phenyl}-1,3,5-triazine-2,4-diamine (12e)

Compound **12e** was prepared with a yield of 18% from **3a** and **11e** using a procedure similar to that described for **12a**. ^{1}H NMR ($CDCl_3$): δ 1.27 (3H, t, J = 7.4 Hz), 1.49–1.78 (2H,

m), 1.89–2.01 (2H, m), 2.20–2.80 (11H, m), 2.30 (3H, s), 3.17 (2H, q, *J* = 7.5 Hz), 3.64–3.75 (2H, m), 3.88 (3H, s), 6.46–6.60 (2H, m), 7.17–7.28 (1H, m), 7.43–7.70 (2H, m), 7.92 (1H, dd, *J* = 1.4, 7.8 Hz), 8.03–8.15 (1H, m), 8.27–8.60 (2H, m), 9.14 (1H, s); MS (ESI) *m/z* $[M+H]^+$ 567; HRMS (ESI) *m/z* Calcd for $C_{28}H_{39}N_8O_3S$ $[M+H]^+$: 567.2866, Found: 567.2868.

***N*-{3-Methoxy-4-[4-(4-methylpiperazin-1-yl)piperidin-1-yl]phenyl}-*N*'-[2-(propane-2-sulfonyl)phenyl]-1,3,5-triazine-2,4-diamine (12f)**

Compound **12f** was prepared with a yield of 56% from **6** and **11a** using a procedure similar to that described for **12a**. ^{1}H NMR ($CDCl_3$): δ 1.31 (6H, d, *J* = 6.8 Hz), 1.73–1.97 (4H, m), 2.30 (3H, s), 2.35–2.79 (11H, m), 3.17–3.32 (1H, m), 3.47–3.58 (2H, m), 3.87 (3H, s), 6.80–7.70 (6H, m), 7.88 (1H, dd, *J* = 1.6, 8.0 Hz), 8.35–8.50 (1H, br), 8.53–8.64 (1H, m), 9.26–9.62 (1H, br); MS (ESI) *m/z* $[M+H]^+$ 581; HRMS (ESI) *m/z* Calcd for $C_{29}H_{41}N_8O_3S$ $[M+H]^+$: 581.3022, Found: 581.3020.

***N*-{4-[4-(4-Methylpiperazin-1-yl)piperidin-1-yl]phenyl}-*N*'-[2-(propane-2-sulfonyl)phenyl]-1,3,5-triazine-2,4-diamine (12g)**

Compound **12g** was prepared with a yield of 38% from **3b** and **11a** using a procedure similar to that described for **12a**. ^{1}H NMR ($CDCl_3$): δ 1.31 (6H, d, *J* = 6.8 Hz), 1.49–1.78 (2H, m), 1.90–2.01 (2H, m), 2.30 (3H, s), 2.24–2.86 (11H, m), 3.18–3.31 (1H, m), 3.66–3.79 (2H,

m), 6.87–7.16 (3H, m), 7.17–7.24 (1H, m), 7.33–7.48 (2H, m), 7.49–7.71 (1H, br), 7.88 (1H, dd, *J* = 1.6, 8.0 Hz), 8.29–8.47 (1H, br), 8.48–8.61 (1H, m), 9.24–9.43 (1H, br); MS (ESI) *m/z* $[M+H]^+$ 551; HRMS (ESI) *m/z* Calcd for $C_{28}H_{39}N_8O_2S$ $[M+H]^+$: 551.2917, Found: 551.2926.

***N*-{2-Methyl-4-[4-(4-methylpiperazin-1-yl)piperidin-1-yl]phenyl}-*N*'-[2-(propane-2-sulfonyl)phenyl]-1,3,5-triazine-2,4-diamine (12h)**

Compound **12h** was prepared from **3c**, which was obtained from **2c**, and **11a** using a procedure similar to that described for **12a** (13% in two steps from **2c**). ^{1}H NMR ($CDCl_3$): δ 1.31 (6H, d, *J* = 6.8 Hz), 1.50–1.80 (2H, m), 1.88–2.02 (2H, m), 2.21–2.87 (11H, m), 2.25 (3H, s), 2.30 (3H, s), 3.15–3.33 (1H, m), 3.68–3.80 (2H, m), 6.48–7.75 (6H, m), 7.78–7.94 (1H, m), 8.30–8.70 (2H, m), 9.24–9.45 (1H, br); MS (ESI) *m/z* $[M+H]^+$ 565; HRMS (ESI) *m/z* Calcd for $C_{29}H_{41}N_8O_2S$ $[M+H]^+$: 565.3073, Found: 565.3077.

***N*-{2-Ethoxy-4-[4-(4-methylpiperazin-1-yl)piperidin-1-yl]phenyl}-*N*'-[2-(propane-2-sulfonyl)phenyl]-1,3,5-triazine-2,4-diamine (12i)**

Compound **12i** was prepared from **3d**, which was obtained from **2d**, and **11a** using a procedure similar to that described for **12a** (11% in two steps from **2d**). ^{1}H NMR ($CDCl_3$): δ 1.31 (6H, d, *J* = 6.8 Hz), 1.46 (3H, t, *J* = 7.0 Hz), 1.53–1.79 (2H, m), 1.88–2.00 (2H, m), 2.24–2.79 (11H, m), 2.30 (3H, s), 3.18–3.32 (1H, m), 3.60–3.74 (2H, m), 4.10 (2H, q, *J* = 7.1 Hz),

6.45–6.59 (2H, m), 7.16–7.29 (1H, m), 7.47–7.70 (2H, m), 7.89 (1H, dd, *J* = 1.6, 8.0 Hz), 8.04–8.20 (1H, m), 8.27–8.48 (1H, br), 8.49–8.60 (1H, m), 9.22–9.34 (1H, br); MS (ESI) *m/z* $[M+H]^+$ 595; HRMS (ESI) *m/z* Calcd for $C_{30}H_{43}N_8O_3S$ $[M+H]^+$: 595.3179, Found: 595.3180.

***N*-{4-[4-(4-Methylpiperazin-1-yl)piperidin-1-yl]-2-(propan-2-yloxy)phenyl}-*N*'-[2-(propane-2-sulfonyl)phenyl]-1,3,5-triazine-2,4-diamine (12j)**

Compound **12j** was prepared from **3e**, which was obtained from **2e**, and **11a** using a procedure similar to that described for **12a** (9% in two steps from **2e**). ^{1}H NMR ($CDCl_3$): δ 1.31 (6H, d, *J* = 6.8 Hz), 1.38 (6H, d, *J* = 6.0 Hz), 1.48–1.79 (2H, m), 1.86–2.02 (2H, m), 2.23–2.80 (11H, m), 2.31 (3H, s), 3.18–3.34 (1H, m), 3.59–3.74 (2H, m), 4.52–4.66 (1H, m), 6.44–6.60 (2H, m), 7.15–7.29 (1H, m), 7.50–7.71 (2H, m), 7.89 (1H, dd, *J* = 1.4, 7.8 Hz), 8.05–8.24 (1H, m), 8.30–8.47 (1H, br), 8.49–8.60 (1H, m), 9.19–9.36 (1H, br); MS (ESI) *m/z* $[M+H]^+$ 609; HRMS (ESI) *m/z* Calcd for $C_{31}H_{45}N_8O_3S$ $[M+H]^+$: 609.3335, Found: 609.3335.

***N*-[2-Methoxy-4-(4-methylpiperazin-1-yl)phenyl]-*N*'-[2-(propane-2-sulfonyl)phenyl]-1,3,5-triazine-2,4-diamine (12k)**

Compound **12k** was prepared with a yield of 39% from 2-methoxy-4-(4-methylpiperazin-1-yl)aniline and **11a** using a procedure similar to that described for **12a**. ^{1}H NMR ($CDCl_3$): δ 1.31 (6H, d, *J* = 6.8 Hz), 2.40 (3H, s), 2.54–2.73 (4H, m), 3.16–3.32 (5H, m),

3.89 (3H, s), 6.46–6.60 (2H, m), 7.16–7.29 (1H, m), 7.47–7.73 (2H, m), 7.88 (1H, dd, *J* = 1.6, 8.0 Hz), 8.04–8.18 (1H, m), 8.26–8.65 (2H ,m), 9.29 (1H, s); MS (ESI) *m/z* $[M+H]^+$ 498; HRMS (ESI) *m/z* Calcd for $C_{24}H_{32}N_7O_3S$ $[M+H]^+$: 498.2287, Found: 498.2279.

***N*-(4-{Ethyl[2-(4-methylpiperazin-1-yl)ethyl]amino}-2-methoxyphenyl)-*N*'-[2-(propane-2-sulfonyl)phenyl]-1,3,5-triazine-2,4-diamine (12l)**

Compound **12l** was prepared from **8**, which was obtained from **7**, and **11a** using a procedure similar to that described for **12a** (16% in two steps from **7**). ^1H NMR ($CDCl_3$): δ 1.18 (3H, t, *J* = 7.0 Hz), 1.31 (6H, d, *J* = 6.8 Hz), 2.30 (3H, s), 2.34–2.77 (10H, m), 3.18–3.31 (1H, m), 3.32–3.52 (4H, m), 3.87 (3H, s), 6.24–6.38 (2H, m), 7.10–7.24 (1H, m), 7.32–7.75 (2H, m), 7.82–8.10 (2H, m), 8.26–8.67 (2H, m), 9.19–9.33 (1H, br); MS (ESI) *m/z* $[M+H]^+$ 569; HRMS (ESI) *m/z* Calcd for $C_{28}H_{41}N_8O_3S$ $[M+H]^+$: 569.3022, Found: 569.3014.

1-Nitro-3-(propan-2-ylsulfanyl)benzene (14)

A mixture of 1,1'-disulfanediylbis(3-nitrobenzene) (**13**, 3.00 g, 9.73 mmol) and K_2CO_3 (2.69 g, 19.5 mmol) in DMF (200 mL) was stirred at room temperature for 2 min. To this mixture were added 2-bromopropane (2.01 mL, 21.4 mmol), sodium hydroxymethanesulfinate (3.45 g, 29.2 mmol) and H_2O (3 mL), and the reaction mixture was stirred at room temperature for 2 h. Water was added to this mixture, and the resulting slurry was extracted with Et_2O. The

organic layer was washed with brine, dried over anhydrous $MgSO_4$, and concentrated *in vacuo* to give **14** (2.95 g, 77%) as a yellow oil. ^{1}H NMR ($CDCl_3$): δ 1.32–1.40 (6H, m), 3.45–3.61 (1H, m), 7.41–7.52 (1H, m), 7.62–7.70 (1H, m), 8.01–8.09 (1H, m), 8.17–8.24 (1H, m); MS (EI) *m/z* $[M]^+$ 197.

1-Nitro-3-(propane-2-sulfonyl)benzene (15)

To a solution of 1-nitro-3-(propan-2-ylsulfanyl)benzene (**14**, 2.95 g, 15.0 mmol) in $CHCl_3$ (60 mL) was added mCPBA (contains ca. 25% water, 8.60 g, 37.4 mmol), and the reaction mixture was stirred at room temperature for 2 h, then at 50 °C for 12 h. Saturated aqueous $NaHCO_3$ solution (100 mL) and 5% aqueous sodium sulfite solution (100 mL) were added to this mixture, and the resulting slurry was extracted with $CHCl_3$. The organic layer was washed with saturated aqueous $NaHCO_3$ solution and brine, dried over Na_2SO_4, and concentrated *in vacuo* to give **15** (3.38 g, 99%) as a white solid. ^{1}H NMR (DMSO-d_6): δ 1.19 (6H, d, J = 6.8 Hz), 3.57–3.70 (1H, m), 7.92–8.04 (1H, m), 8.27–8.37 (1H, m), 8.50–8.56 (1H, m), 8.56–8.65 (1H, m); MS (CI) *m/z* $[M+H]^+$ 230.

3-(Propane-2-sulfonyl)aniline (16)

To a mixture of 1-nitro-3-(propane-2-sulfonyl)benzene (**15**, 3.38 g, 14.3 mmol) and AcOH (35 mL) was added iron powder (2.64 g, 47.2 mmol), and the reaction mixture was

stirred at 80 °C for 3 h. To this mixture was added EtOAc; the insoluble material was removed by filtration, and the filtrate was concentrated *in vacuo*. To the residue was added EtOAc, and the insoluble material was again removed by filtration. The organic layer was washed with water, saturated aqueous $NaHCO_3$ solution and brine, dried over Na_2SO_4, and concentrated *in vacuo*. The residue was purified by silica gel column chromatography ($CHCl_3$/MeOH = 100:0 to 50:1) to give **16** (1.79 g, 63%) as a pale yellow solid. ^{1}H NMR ($CDCl_3$): δ 1.30 (6H, d, *J* = 6.8 Hz), 3.10–3.26 (1H, m), 3.82–4.08 (2H, br), 6.86–6.96 (1H, m), 7.13–7.18 (1H, m), 7.19–7.25 (1H, m), 7.25–7.36 (1H, m); MS (EI) *m/z* $[M]^+$ 199.

4-Chloro-*N*-[3-(propane-2-sulfonyl)phenyl]-1,3,5-triazin-2-amine (**17**)

Compound **17** was prepared with a yield of 92% from **9a** and **16** using a procedure similar to that described for **11d**. ^{1}H NMR ($CDCl_3$): δ 1.35 (6H, d, *J* = 6.8 Hz), 3.18–3.33 (1H, m), 7.54–7.65 (1H, m), 7.66–7.74 (1H, m), 7.76–8.00 (2H, m), 8.01–8.34 (1H, br), 8.49–8.72 (1H, br); MS (ESI) *m/z* $[M+H]^+$ 313.

***N*-{2-Methoxy-4-[4-(4-methylpiperazin-1-yl)piperidin-1-yl]phenyl}-*N*'-[3-(propane-2-sulfonyl)phenyl]-1,3,5-triazine-2,4-diamine** (**18**)

Compound **18** was prepared with a yield of 36% from **3a** and **17** using a procedure similar to that described for **12a**. ^{1}H NMR ($CDCl_3$): δ 1.32 (6H, d, *J* = 6.8 Hz), 1.51–1.78 (2H,

m), 1.88–2.01 (2H, m), 2.30 (3H, s), 2.33–2.80 (11H, m), 3.12–3.29 (1H, m), 3.63–3.75 (2H, m), 3.87 (3H, s), 6.48–6.61 (2H, m), 7.16–7.36 (1H, m), 7.45–7.62 (2H, m), 7.85–8.25 (3H, m), 8.30–8.44 (1H, br); MS (ESI) *m/z* $[M+H]^+$ 581; HRMS (ESI) *m/z* Calcd for $C_{29}H_{41}N_8O_3S$ $[M+H]^+$: 581.3022, Found: 581.3033.

8-(3-Methoxy-4-nitrophenyl)-1,4-dioxa-8-azaspiro[4.5]decane (**19**)

To a mixture of 4-fluoro-2-methoxy-1-nitrobenzene (**1a**, 15 g, 87.7 mmol) and K_2CO_3 (30.0 g, 217 mmol) in DMF (150 mL) was added 1,4-dioxa-8-azaspiro[4.5]decane (15 g, 105 mmol), and the reaction mixture was stirred at 70 °C overnight. The insoluble material was removed by filtration, and ice water was added to the filtrate. The resulting solid was filtered and washed with Et_2O to give **19** (23.8 g, 92%) as a yellow solid. ^{1}H NMR ($CDCl_3$): δ 1.78–1.85 (4H, m), 3.51–3.59 (4H, m), 3.95 (3H, s), 4.01 (4H, s), 6.33 (1H, d, *J* = 2.8 Hz), 6.43 (1H, dd, *J* = 2.4, 9.2 Hz), 8.00 (1H, d, *J* = 9.2 Hz); MS (ESI) *m/z* $[M+H]^+$ 295.

4-(1,4-Dioxa-8-azaspiro[4.5]decan-8-yl)-2-methoxyaniline (**20**)

Compound **20** was prepared with a yield of 82% from **19** using a procedure similar to that described for **3a**. ^{1}H NMR ($CDCl_3$): δ 1.83–1.94 (4H, m), 3.10–3.22 (4H, m), 3.45–3.65 (2H, br), 3.83 (3H, s), 3.99 (4H, s), 6.45 (1H, dd, *J* = 2.4, 8.4 Hz), 6.55 (1H, d, *J* = 2.4 Hz), 6.63 (1H, d, *J* = 8.4 Hz); MS (ESI) *m/z* $[M+H]^+$ 265.

***N*-[4-(1,4-Dioxa-8-azaspiro[4.5]decan-8-yl)-2-methoxyphenyl]-*N*'-[2-(propane-2-sulfonyl)phenyl]-1,3,5-triazine-2,4-diamine (21)**

A mixture of 4-chloro-*N*-[2-(propane-2-sulfonyl)phenyl]-1,3,5-triazin-2-amine (**11a**, 1.00 g, 3.20 mmol), 4-(1,4-dioxa-8-azaspiro[4.5]decan-8-yl)-2-methoxyaniline (**20**, 845 mg, 3.20 mmol) and DIPEA (0.56 mL, 3.20 mmol) in NMP (3.5 mL) was irradiated with microwaves at 120 °C for 40 min. Water was added to this reaction mixture, and the resulting solid was filtered and dried to give **21** (1.62 g, 94%). ^{1}H NMR ($CDCl_3$): δ 1.31 (6H, d, J = 6.8 Hz), 1.80–1.92 (4H, m), 3.18–3.35 (5H, m), 3.88 (3H, s), 4.01 (4H, s), 6.48–6.62 (2H, m), 7.17–7.31 (1H, m), 7.43–7.70 (2H, m), 7.82–7.95 (1H, m), 8.03–8.18 (1H, m), 8.28–8.64 (2H, m), 9.25–9.32 (1H, br); MS (ESI) *m/z* $[M+H]^+$ 541.

1-[3-Methoxy-4-({4-[2-(propane-2-sulfonyl)anilino]-1,3,5-triazin-2-yl}amino)phenyl]piperidin-4-one (22)

A mixture of *N*-[4-(1,4-dioxa-8-azaspiro[4.5]decan-8-yl)-2-methoxyphenyl]-*N*'-[2-(propane-2-sulfonyl)phenyl]-1,3,5-triazine-2,4-diamine (**21**, 2.27 g, 4.20 mmol) and 4 M aqueous HCl solution (24 mL) in 1,4-dioxane (20 mL) was stirred at 80 °C for 2 h. The reaction mixture was concentrated *in vacuo*, and saturated aqueous $NaHCO_3$ solution was added to the residue. The resulting slurry was extracted with $CHCl_3$. The organic layer was washed with

brine, dried over anhydrous $MgSO_4$, and concentrated *in vacuo*. The residue was purified by silica gel column chromatography ($CHCl_3$/MeOH = 100:0 to 20:1) to give **22** (1.49 g, 71%). ^{1}H NMR ($CDCl_3$): δ 1.32 (6H, d, *J* = 6.8 Hz), 2.51–2.68 (4H, m), 3.18–3.34 (1H, m), 3.52–3.68 (4H, m), 3.91 (3H, s), 6.51–6.68 (2H, m), 7.17–7.74 (3H, m), 7.84–7.95 (1H, m), 8.04–8.26 (1H, m), 8.30–8.68 (2H, m), 9.24–9.38 (1H, m); MS (ESI) *m/z* $[M+H]^+$ 497.

_N_-{2-Methoxy-4-[4-(morpholin-4-yl)piperidin-1-yl]phenyl}-_N'_-[2-(propane-2-sulfonyl)phenyl]-1,3,5-triazine-2,4-diamine trihydrochloride (**23**)

To a solution of 1-[3-methoxy-4-({4-[2-(propane-2-sulfonyl)anilino]-1,3,5-triazin-2-yl}amino)phenyl]piperidin-4-one (**22**, 200 mg, 0.403 mmol) in dichloromethane were added morpholine (0.14 mL, 1.61 mmol) and sodium triacetoxyborohydride (128 mg, 0.604 mmol), and the reaction mixture was stirred at room temperature for 2 h. Water and saturated aqueous $NaHCO_3$ solution were added to the mixture, and the resulting slurry was extracted with $CHCl_3$. The organic layer was washed with brine, dried over anhydrous $MgSO_4$, and concentrated *in vacuo*. The residue was purified by silica gel column chromatography ($CHCl_3$/MeOH = 100:0 to 10:1). The obtained product was dissolved in THF and treated with 4 M HCl in EtOAc, and then the mixture was concentrated *in vacuo*. The residue was treated with acetonitrile, EtOH and water to give **23** (133 mg, 49%). ^{1}H NMR (DMSO-d_6): δ 1.15 (6H, d, *J* = 6.8 Hz), 1.82–2.06 (2H, m), 2.18–2.31 (2H, m), 2.78–3.01 (2H, m), 3.01–3.21 (2H, m), 3.29–3.55 (4H, m),

3.80 (3H, s), 3.82–4.06 (6H, m), 6.57–6.99 (2H, m), 7.27–7.47 (2H, m), 7.55–7.91 (2H, m), 8.12–8.64 (2H, m), 9.25 (1H, s), 9.51 (1H, s), 11.08–11.35 (1H, br); MS (ESI) *m/z* $[M+H]^+$ 568; *Anal*. Calcd for $C_{28}H_{37}N_7O_4S.2.8HCl.H_2O$: C, 48.89; H, 6.13; N, 14.25; S, 4.66; Cl, 14.43. Found: C, 48.62; H, 6.05; N, 14.14; S, 4.73; Cl, 14.43.

***tert*-Butyl 4-[3-methoxy-4-({4-[2-(propane-2-sulfonyl)anilino]-1,3,5-triazin-2-yl}amino)phenyl]piperidine-1-carboxylate (25)**

A mixture of 4-chloro-*N*-[2-(propane-2-sulfonyl)phenyl]-1,3,5-triazin-2-amine (**11a**, 700 mg, 2.24 mmol), *tert*-butyl 4-(4-amino-3-methoxyphenyl)piperidine-1-carboxylate (**24**, 686 mg, 2.24 mmol) and DIPEA (0.47 mL, 2.69 mmol) in NMP (4 mL) was irradiated with microwaves at 120 °C for 20 min. Water was added to this reaction mixture, and the resulting solid was filtered and dried *in vacuo*. This solid was dissolved in EtOAc, and the organic layer was dried over anhydrous $MgSO_4$, then concentrated *in vacuo*. The residue was purified by silica gel column chromatography (*n*-hexane/EtOAc = 100:0 to 50:50) to give **25** (960 mg, 74%). ^1H NMR ($CDCl_3$): δ 1.31 (6H, d, *J* = 6.8 Hz), 1.49 (9H, s), 1.53–1.71 (2H, m), 1.77–1.90 (2H, m), 2.58–2.70 (1H, m), 2.73–2.91 (2H, m), 3.18–3.32 (1H, m), 3.91 (3H, s), 4.16–4.37 (2H, m), 6.74–6.78 (1H, m), 6.80–6.86 (1H, m), 7.21–7.30 (1H, m), 7.53–7.79 (2H, m), 7.86–7.94 (1H, m), 8.26 (1H, d, *J* = 8.4 Hz), 8.35–8.60 (2H, m), 9.33 (1H, s); MS (ESI) *m/z* $[M+H]^+$ 583.

***N*-[2-Methoxy-4-(piperidin-4-yl)phenyl]-*N*'-[2-(propane-2-sulfonyl)phenyl]-1,3,5-triazine-2,4-diamine (26)**

To a solution of *tert*-butyl 4-[3-methoxy-4-({4-[2-(propane-2-sulfonyl)anilino]-1,3,5-triazin-2-yl}amino)phenyl]piperidine-1-carboxylate (**25**, 980 mg, 1.68 mmol) in EtOAc (10 mL) and MeOH (10 mL) was added 4 M HCl in EtOAc (20 mL). After stirring at room temperature for 1 h, the mixture was concentrated *in vacuo*. Saturated aqueous $NaHCO_3$ solution was added to the residue, and the resulting slurry was extracted with $CHCl_3$. The organic layer was washed with brine, dried over anhydrous $MgSO_4$, and concentrated *in vacuo* to give **26** (840 mg, quantitative). ^{1}H NMR ($CDCl_3$): δ 1.31 (6H, d, J = 6.8 Hz), 1.68–2.30 (4H, m), 2.58–2.71 (1H, m), 2.74–2.90 (2H, m), 3.17–3.37 (3H, m), 3.91 (3H, s), 6.77–6.82 (1H, m), 6.82–6.90 (1H, m), 7.20–7.29 (1H, m), 7.49–7.83 (2H, m), 7.89 (1H, dd, J = 1.6, 8.0 Hz), 8.25 (1H, d, J = 8.0 Hz), 8.33–8.48 (1H, br), 8.48–8.62 (1H, m), 8.90–9.70 (1H, br); MS (ESI) *m/z* $[M+H]^+$ 483.

***N*-[2-Methoxy-4-(1'-methyl[1,4'-bipiperidin]-4-yl)phenyl]-*N*'-[2-(propane-2-sulfonyl)phenyl]-1,3,5-triazine-2,4-diamine (27)**

A mixture of *N*-[2-methoxy-4-(piperidin-4-yl)phenyl]-*N*'-[2-(propane-2-sulfonyl)phenyl]-1,3,5-triazine-2,4-diamine (**26**, 300 mg, 0.622 mmol), 1-methylpiperidin-4-

one (87 μL, 0.746 mmol) and sodium triacetoxyborohydride (158 mg, 0.746 mmol) in dichloromethane (11 mL) was stirred at room temperature overnight. Water and saturated aqueous $NaHCO_3$ solution were added to the reaction mixture, and the resulting slurry was extracted with $CHCl_3$. The organic layer was washed with brine, dried over anhydrous $MgSO_4$, and concentrated *in vacuo*. The residue was purified by silica gel column chromatography ($CHCl_3$/MeOH/28% aqueous NH_3 = 100:0:0 to 10:1:0.1) to give **27** (140 mg, 39%). ^{1}H NMR ($CDCl_3$): δ 1.31 (6H, d, *J* = 6.8 Hz), 1.49–2.04 (10H, m), 2.22–2.40 (3H, m), 2.28 (3H, s), 2.42–2.55 (1H, m), 2.88–2.99 (2H, m), 3.00–3.12 (2H, m), 3.18–3.33 (1H, m), 3.89 (3H, s), 6.77–6.83 (1H, m), 6.83–6.92 (1H, m), 7.19–7.29 (1H, m), 7.53–7.82 (2H, m), 7.89 (1H, dd, *J* = 1.6, 8.0 Hz), 8.22 (1H, d, *J* = 8.4 Hz), 8.34–8.47 (1H, br), 8.47–8.60 (1H, m), 9.31 (1H, s); MS (ESI) *m/z* $[M+H]^+$ 580; HRMS (ESI) *m/z* Calcd for $C_{30}H_{42}N_7O_3S$ $[M+H]^+$: 580.3069, Found: 580.3077.

***In vitro* kinase inhibitory assay**

EML4–ALK variant 1 protein was isolated from Ba/F3 cells transformed with EML4–ALK. Kinase activity was measured using HTRF® KinEASE™-TK (Cisbio Bioassays, Codolet, France). The final concentration of ATP for EML4–ALK variant 1 protein was 100 μM.

***In vitro* cell growth assay**

Ba/F3 cells transformed with EML4–ALK variant 1 were seeded in 96-well plates at 2×10^3 cells per well and treated with various concentrations of compounds (**12a**, **12b**, and **12k**) for 3 days, then cell viability was measured using the CellTiter-Glo™ Luminescent Cell Viability Assay (Promega Corporation, Madison, WI, U.S.A.) or seeded in 384-well plates at 2.5×10^2 or 5×10^2 cells per well, and treated with various concentrations of compounds (**12e**, **12f**, **12i**, **23**, and **27**) for 2 days, then cell viability was measured with alamarBlue® Cell Viability Reagent (Thermo Fisher Scientific Inc., Waltham, MA, U.S.A.).

***In vivo* antitumor test in NCI-H2228 xenograft model** [26]

All experiments were performed in accordance with the regulation of the Animal Ethics Committee of Astellas Pharma Inc.

NCI-H2228 cells were subcutaneously inoculated into the flank of male NOD-SCID mice (NOD.CB17-*Prkdc*^{scid}/J, Charles River Laboratories Japan, Inc., Kanagawa, Japan) at

5×10^6 cells/0.1 mL/mouse. Compound **12a** was suspended in 0.5% methylcellulose solution and orally administered once daily. Tumor diameter was measured using a caliper, and tumor volume was determined by calculating the volume of an ellipsoid using the following formula: length × width^2 × 0.5.

Computational Modeling

Docking simulation of **12a** with wild-type ALK was performed using the docking software GLIDE (Schrödinger, LLC, New York, NY, U.S.A.). The coordinate of wild-type ALK with NVP-TAE684 (PDB ID: 2XB7 [36]) was used as a template for the docking, and hydrogen atoms were added using the modeling software MOE with the function Protonate3D (Chemical Computing Group Inc., Montreal, Quebec, Canada). The docking mode with the highest docking score was employed.

Chapter 2: Synthesis and structure–activity relationships of pyrazine-2-carboxamide derivatives

1. Introduction

In Chapter 1, I described the discovery of compound **12a** (Figure 6), a 1,3,5-triazine derivative, as a novel EML4–ALK inhibitor. After the identification of **12a**, the next objective was to identify a more potent EML4–ALK inhibitor with a different chemical structure to that of 1,3,5-triazine derivatives. Screening of a compound library and a subsequent preliminary SAR exploration led to the identification of compound **30a**, which has a pyrazine-2-carboxamide substructure (Figure 8). Structural optimization of each component of pyrazine-2-carboxamide derivative compounds resulted in the identification of compound **37c** [37]. Here, I describe the synthesis and biological evaluation of pyrazine-2-carboxamide derivatives [38, 39], along with studies on their SAR using computational modeling.

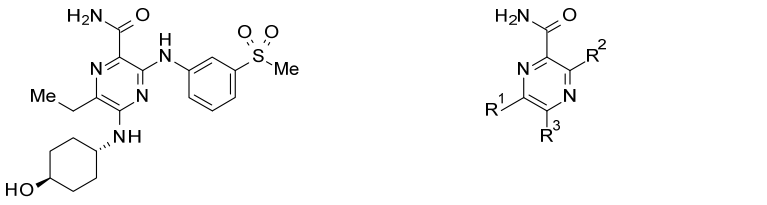

30a pyrazine−2−carboxamide substructure

Figure 8. Structures of **30a** and the pyrazine-2-carboxamide substructure.

2. Results and discussion

2.1. Chemistry

The synthesis of compounds **30a**–**c** and **30d** is shown in Scheme 8 and Scheme 9, respectively. Compounds **30a**–**c** were synthesized by reacting **28a**–**c** [40] with 3-(methanesulfonyl)aniline, followed by introducing (1*r*,4*r*)-4-aminocyclohexan-1-ol. Compound **30d** was prepared from **28d** [40] by employing procedures similar to those described for **30a**–**c**.

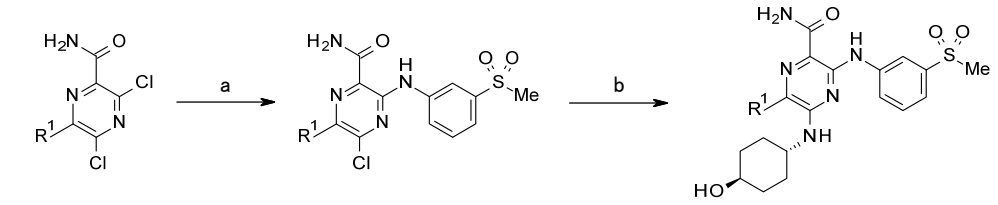

28a : R¹ = Et
28b : R¹ = H
28c : R¹ = *n*–Pr

29a : R¹ = Et (17%)
29b : R¹ = H (55%)
29c : R¹ = *n*–Pr (46%)

30a : R¹ = Et (63%)
30b : R¹ = H (84%)
30c : R¹ = *n*–Pr (54%)

Scheme 8. Synthesis of compounds **30a**–**c**.

Reagents and conditions: (a) 3-(methanesulfonyl)aniline, DIPEA, 1,4-dioxane, 110 °C, sealed tube 170 °C, or sealed tube 170 °C then 180 °C; (b) (1*r*,4*r*)-4-aminocyclohexan-1-ol, NMP, microwave, 190 °C.

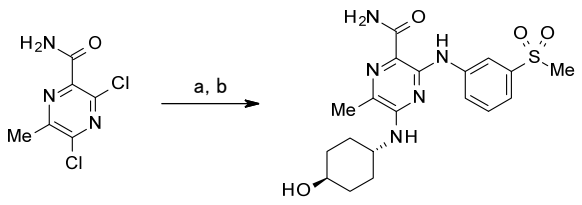

28d **30d**

Scheme 9. Synthesis of compound **30d**.

Reagents and conditions: (a) 3-(methanesulfonyl)aniline, DIPEA, 1,4-dioxane, sealed tube, 170 °C; 3-(methanesulfonyl)aniline, DMI, microwave, 220 °C; (b) (1*r*,4*r*)-4-aminocyclohexan-1-ol, microwave, 190 °C, 31% in 2 steps.

The synthesis of compounds **31**–**33** is shown in Scheme 10. The bromo derivative **31** and chloro derivative **33** were synthesized by introducing a bromo group or chloro group into compound **30b** using *N*-bromosuccinimide (NBS) or *N*-chlorosuccinimide (NCS), respectively. The cyclopropyl derivative **32** was synthesized by the Suzuki–Miyaura coupling reaction using cyclopropylboronic acid, $Pd(PPh_3)_4$, and K_2CO_3 in 1,4-dioxane and water.

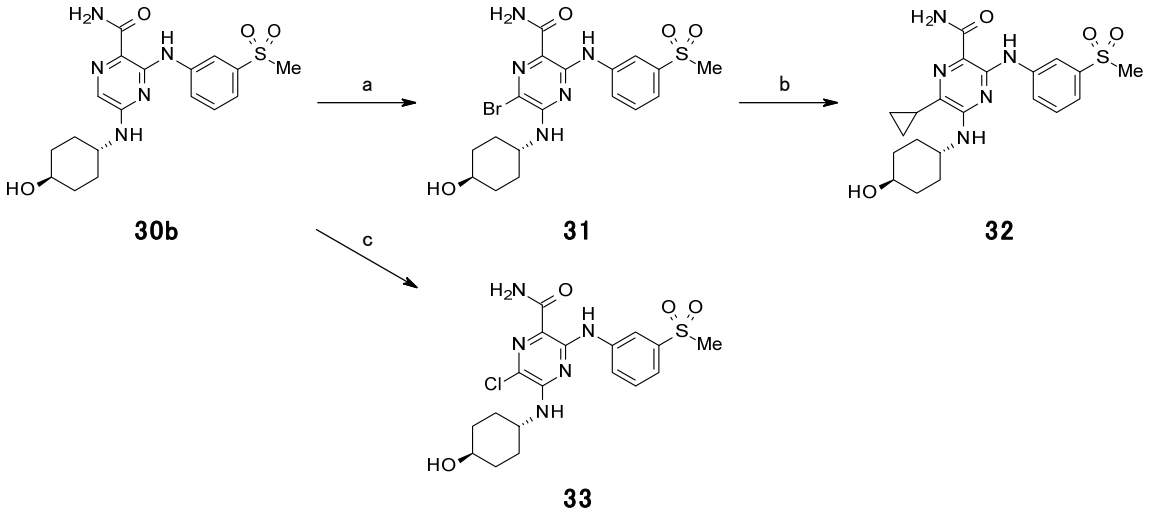

Scheme 10. Synthesis of compounds **31**–**33**.

Reagents and conditions: (a) NBS, $CHCl_3$, MeCN, room temperature, 73%; (b) cyclopropylboronic acid, $Pd(PPh_3)_4$, K_2CO_3, 1,4-dioxane, H_2O, 100 °C then 115 °C, 21%; (c) NCS, $CHCl_3$, MeCN, 70 °C, 58%.

The synthesis of compound **35** is shown in Scheme 11. Compound **35** was synthesized by reacting **28a** [40] with compound **3a**, followed by introducing (1*r*,4*r*)-4-aminocyclohexan-1-ol.

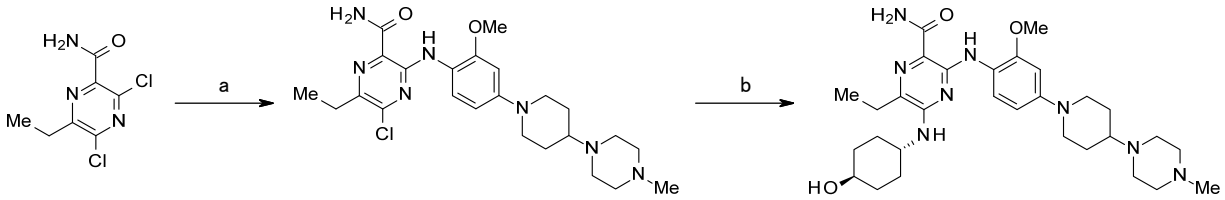

28a **34** **35**

Scheme 11. Synthesis of compound **35**.

Reagents and conditions: (a) **3a**, DIPEA, 1,4-dioxane, 110 °C, 63%; (b) (1*r*,4*r*)-4-aminocyclohexan-1-ol, NMP, microwave, 190 °C, 37%.

The synthesis of compounds **37a**–**f** is shown in Scheme 12. Compounds **37a**–**f** were synthesized by reacting **28a** [40] with compound **6** to obtain compound **36**, followed by introducing the corresponding amines.

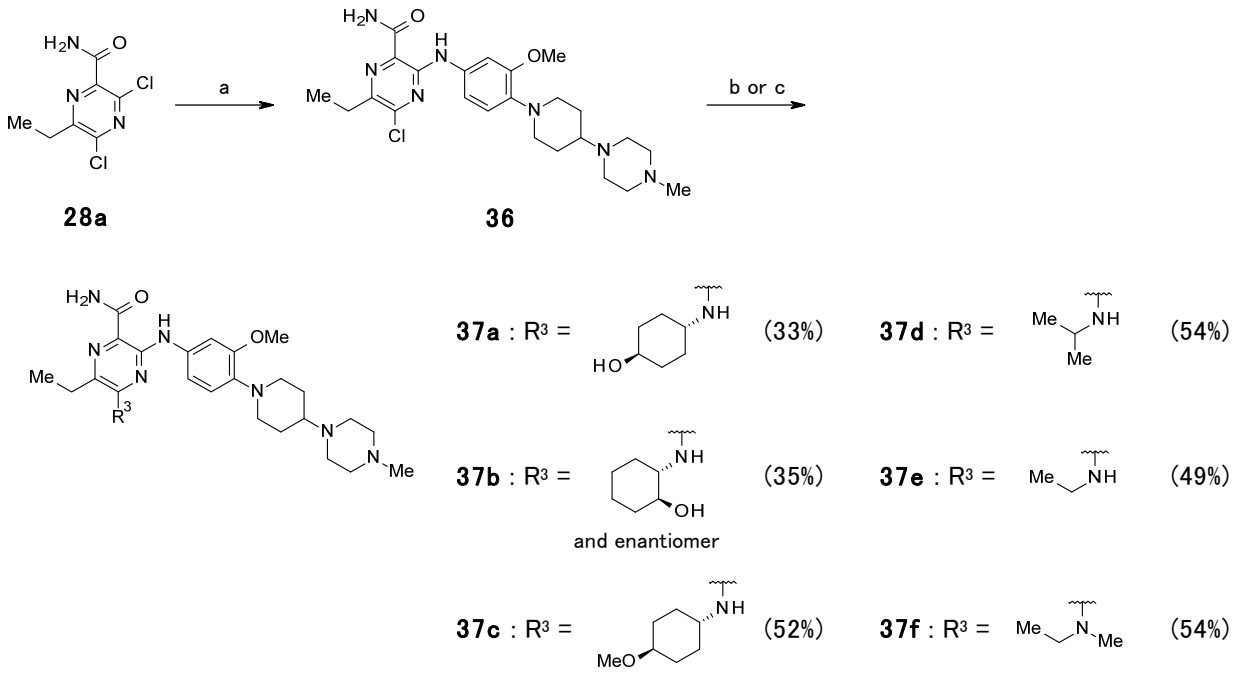

Scheme 12. Synthesis of compounds **37a**–**f**.

Reagents and conditions: (a) **6**, DIPEA, 1,4-dioxane, 110 °C, 55%; (b) amine, NMP, microwave, 190 °C or 200 °C; (c) amine, DIPEA, NMP, microwave, 190 °C.

2.2. Biological evaluation

The synthesized compounds were evaluated using the *in vitro* EML4–ALK inhibitory assay and cell growth assay in Ba/F3 cells expressing EML4–ALK. In addition, selected compounds were evaluated using an *in vivo* antitumor test, aqueous solubility assay and/or permeability assay. The SARs of R^1, R^2, and R^3 components are shown in Tables 5–7, respectively.

Table 5 shows the substituent effects at the ethyl component of **30a**. Replacement of the ethyl group of **30a** with a methyl group (**30d**) resulted in a three-fold reduction in inhibitory activity against EML4–ALK. The unsubstituted compound **30b** showed a 16-fold decrease in inhibitory activity against EML4–ALK compared to that of **30a**. In contrast, the *n*-propyl derivative **30c** and cyclopropyl derivative **32** showed equipotent EML4–ALK inhibitory activity to that of **30a**. The docking model of **30a** with ALK indicated that the ethyl moiety occupied the hydrophobic pocket formed by Val1130, Val1180, Leu1196, and Leu1256 (Figure 9). Therefore, the decrease in inhibitory activity of **30d** and **30b** compared to that of **30a** may be attributed to the reduction or loss of interaction between these compounds and the hydrophobic pocket. In contrast, compounds **30c** and **32** retained their inhibitory activity, possibly because the *n*-propyl group of compound **30c** and cyclopropyl group of compound **32** were able to occupy the hydrophobic pocket. Both the bromo derivative **31** and chloro

derivative **33** showed a five-fold decrease in inhibitory activity against EML4–ALK compared to that of **30a**.

Table 5. Structure–activity relationship of compounds **30a**–**d** and **31**–**33**.

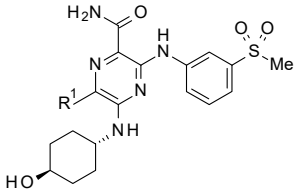

Compound	R^1	EML4–ALK IC_{50} (nM)
30a	Et	17
30d	Me	51
30b	H	270
30c	*n*-Pr	23
32	*c*-Pr	37
31	Br	82
33	Cl	82

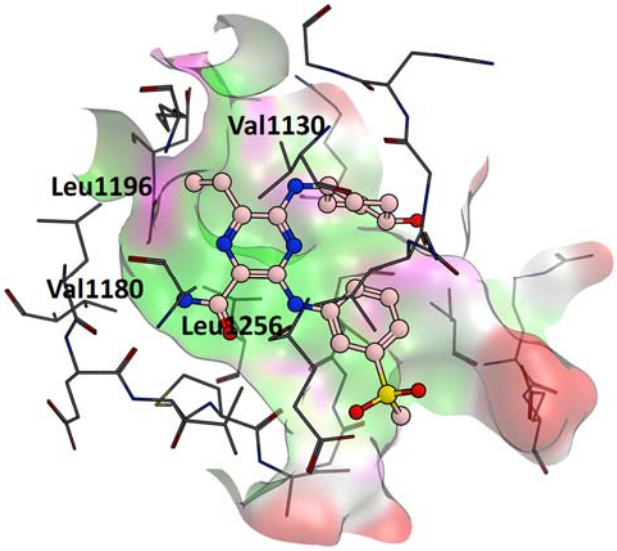

(a)

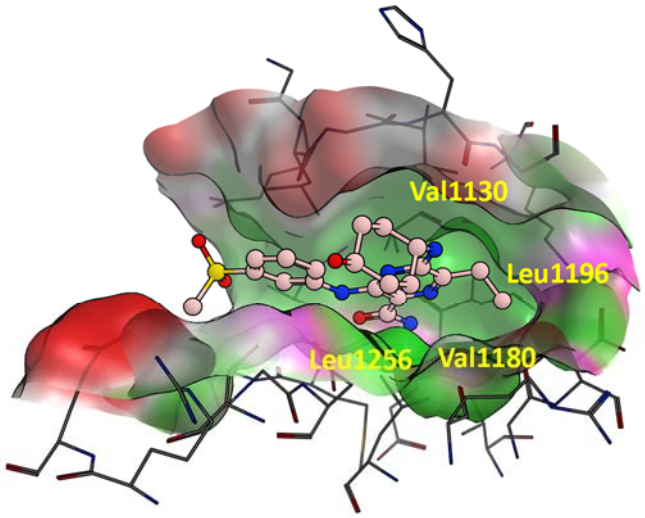

(b)

Figure 9. Molecular modeling of **30a** (pale pink, ball and stick) with human ALK [37].

The protein surface is colored according to the characteristics of the pocket (green: hydrophobic, magenta: polar, red: solvent exposed).

(a) Best docking solution calculated by GLIDE.

(b) The solution shown in (a) from a different angle, focusing on the ethyl moiety.

Table 6 shows the SAR of the 3-(methanesulfonyl)anilino moiety in compound **30a**. As described in Chapter 1, according to the docking model, the 2-methoxy-4-[4-(4-methylpiperazin-1-yl)piperidin-1-yl]anilino component of **12a** extends into the solvent-exposed region (Figure 4). The docking study of **30a** suggested that the 3-(methanesulfonyl)anilino component of **30a** extends into the same region (Figure 10). Consistent with these observations, compound **35** retained inhibitory activity against EML4–ALK with an IC_{50} value of 8.9 nM. Replacement of the 2-methoxy group of compound **35** with a 3-methoxy group (**37a**) enhanced the inhibitory activity by 24-fold in the EML4–ALK inhibitory assay and by 9-fold in the cell growth assay using Ba/F3 cells. These results may be explained by the larger space around the 3-position of **37a** than that around the 2-position suggested by the docking model of **37a** with ALK (Figure 11). Additionally, the 4-(4-methylpiperazin-1-yl)piperidin-1-yl groups in **35** and **37a** contributed to improving the solubility of these compounds.

Table 6. Structure–activity relationship of compounds **30a**, **35**, and **37a**.

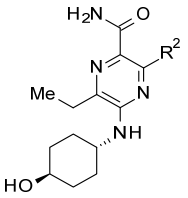

Compound	R^2	EML4–ALK IC_{50} (nM)	Ba/F3 IC_{50} (nM)	Solubility (μM)[a]
30a	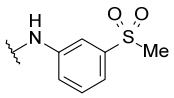	17	68	1.1
35	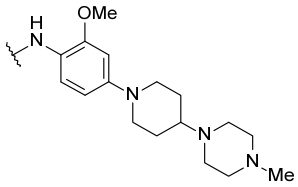	8.9	85	≥100
37a	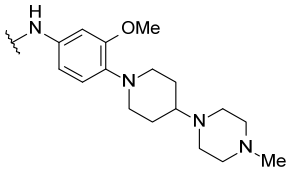	0.37	9.5	≥100

[a] Japanese Pharmacopoeia 2nd fluid for disintegration test (JP2; pH = 6.8 buffer).

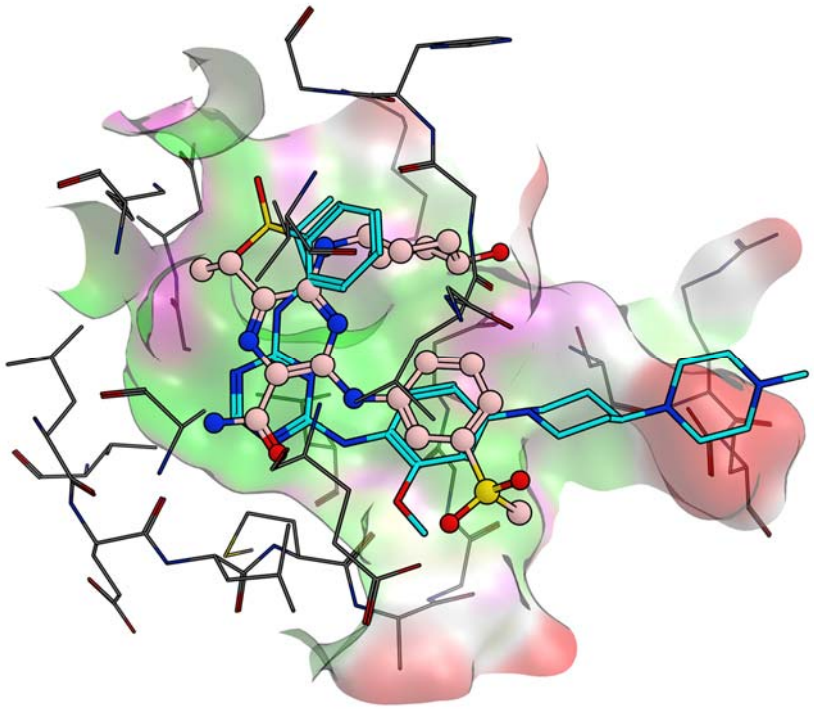

Figure 10. Molecular modeling of **12a** (blue green, stick) and **30a** (pale pink, ball and stick) with human ALK [37].

The protein surface is colored according to the characteristics of the pocket (green: hydrophobic, magenta: polar, red: solvent exposed).

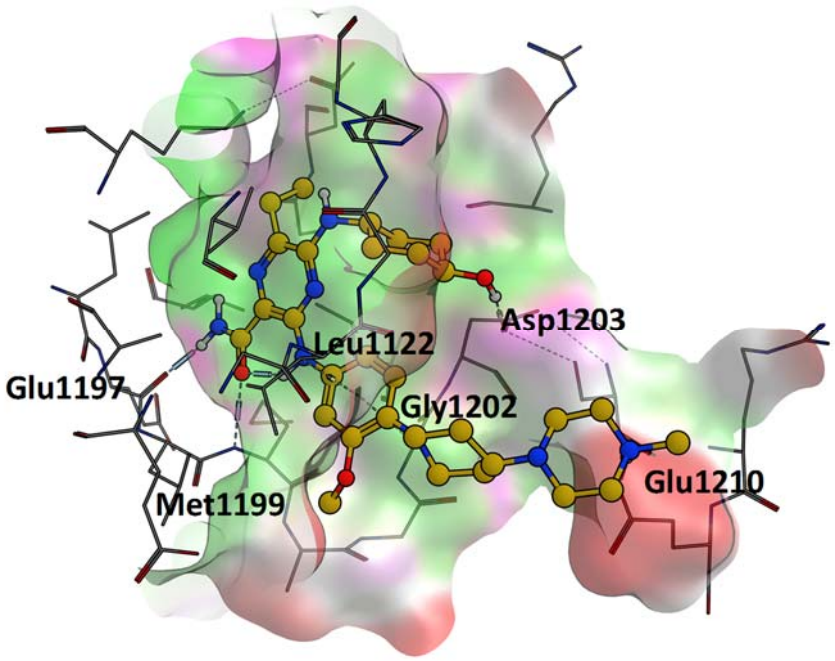

Figure 11. Molecular modeling of **37a** (yellow, ball and stick) with human ALK [37].

The protein surface is colored according to the characteristics of the pocket (green: hydrophobic, magenta: polar, red: solvent exposed).

Table 7 shows the SAR of the amine moiety in **37a**. Compound **37b** showed a decrease in inhibitory activity against EML4–ALK compared to that of **37a**, possibly because the region around the 2-position of the cyclohexyl group is hydrophobic, as shown in the docking model of compound **37a** with ALK (Figure 11). Compound **37c** showed a three-fold decrease in inhibitory activity against EML4–ALK compared to that of **37a**. The docking model of **37a** with ALK indicates that the hydroxy group attached to the cyclohexyl group interacts with Asp1203 (Figure 11). Therefore, the decrease in inhibitory activity of **37c** against EML4–ALK compared to that of **37a** may be due to the loss of this interaction. The alkyl derivatives **37d** and **37e** showed inhibitory activity against EML4–ALK with IC_{50} values of 0.80 nM and 2.5 nM, respectively. Compound **37f** showed a decrease in inhibitory activity against EML4–ALK compared to that of **37e**. These results suggest that the bulkiness around the carbon atom adjacent to the nitrogen atom may contribute to improving inhibitory activity.

Table 7. Structure–activity relationship of compounds **37a**–**f**.

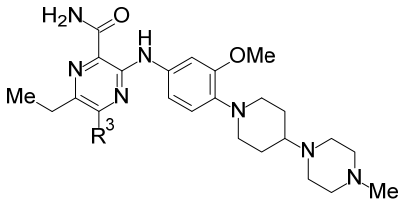

Compound	R^3	EML4–ALK IC_{50} (nM)	Ba/F3 IC_{50} (nM)
37a	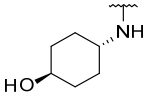	0.37	9.5
37b[a]	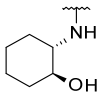	13	48
37c	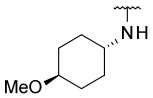	1.0	9.7
37d	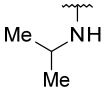	0.80	12
37e	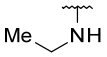	2.5	16
37f	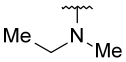	6.6	31

[a] Racemate.

Table 8 shows the antitumor activity of **37a** and **37c**, which demonstrated potent inhibitory activity in the cell growth assay using Ba/F3 cells (IC_{50} < 10 nM), in mice xenografted with 3T3 cells expressing EML4–ALK. Once-daily oral administration of compounds **37a** and **37c** at a dose of 10 mg/kg for 5 days resulted in 34% tumor growth inhibition and 62% tumor regression, respectively. Body weight was not affected in these experiments. As shown in Table 8, the methoxy derivative **37c** showed higher permeability than the hydroxy derivative **37a**, based on findings from the parallel artificial membrane permeability assay (PAMPA). Given these results, I speculated that the potent *in vivo* activity of **37c** compared to that of **37a** may be attributed to the improved drug exposure associated with higher permeability. In addition, the improved permeability of the methoxy derivative **37c** compared to the hydroxy derivative **37a** may explain the finding that **37c** retained inhibitory activity in the cell growth assay compared to **37a** despite **37c** showing a decrease in inhibitory activity against EML4–ALK compared to **37a**, as indicated in Table 7.

Figure 12 shows the antitumor activity of **12a** and **37c** in 3T3 xenograft model mice. Once-daily oral administration of **12a** at a dose of 10 mg/kg for 5 days resulted in 81% tumor growth inhibition. Body weight was not affected in this experiment. Therefore, the antitumor activity of **37c**, which induced tumor regression, was more potent than that observed for **12a**.

Table 8. Antitumor activity of **37a** and **37c** in 3T3 xenograft model mice.

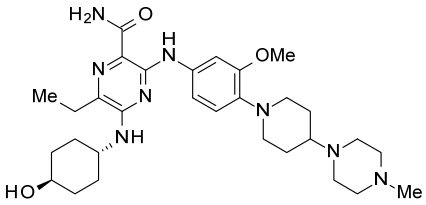

37a

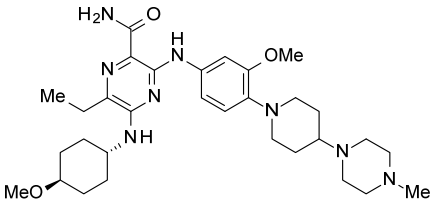

37c

Compound	EML4–ALK IC_{50} (nM)	Ba/F3 IC_{50} (nM)	*In vivo* 3T3 antitumor activity[a]	Permeability ($x10^{-6}$ cm/sec)[b]
37a	0.37	9.5	34% inhibition	1.1
37c	1.0	9.7	62% regression	21

[a] Once-daily oral administration at a dose of 10 mg/kg for 5 days.

[b] Parallel artificial membrane permeability assay (PAMPA) at pH = 6.5.

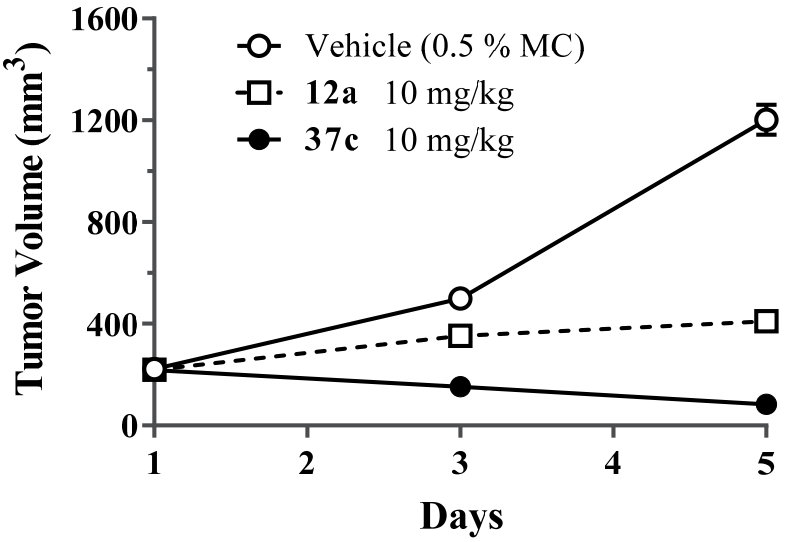

Figure 12. Antitumor activity of **12a** and **37c** in 3T3 xenograft model mice [37].

Mice subcutaneously xenografted with 3T3 cells expressing EML4–ALK were treated with once-daily oral administration of **12a** and **37c** at a dose of 10 mg/kg for 5 days. Each point represents the mean ± SEM of 4 mice in each group.

3. Experimental section

Chemistry

^{1}H NMR spectra were recorded on JEOL JNM-AL400, Varian 400 MR, Varian VNS-400 or Bruker Avance III HD500 spectrometers. Chemical shifts were expressed in δ (ppm) values with tetramethylsilane as an internal reference (s = singlet, d = doublet, t = triplet, q = quartet, m = multiplet, and dd = doublet of doublets). Mass spectra (MS) were recorded on Thermo Electron LCQ Advantage, Waters UPLC/SQD, Waters Alliance HT-ZMD LC/MS system or JEOL GCmateII. Electrospray ionization (ESI) positive high resolution mass spectrum (HRMS) was obtained using Thermo Fisher Exactive Plus Orbitrap.

5-Chloro-6-ethyl-3-[3-(methanesulfonyl)anilino]pyrazine-2-carboxamide (**29a**)

A mixture of 3,5-dichloro-6-ethylpyrazine-2-carboxamide (**28a**, 100 mg, 0.454 mmol), 3-(methanesulfonyl)aniline (78 mg, 0.456 mmol), DIPEA (80 μL, 0.459 mmol) and 1,4-dioxane (3 mL) in a sealed tube was stirred at 170 °C for 15 h. After the mixture was cooled, water was added, and the resulting slurry was extracted with EtOAc. The organic layer was washed with brine, dried over anhydrous $MgSO_4$, and concentrated *in vacuo*. The resulting product was washed with $CHCl_3$ and the obtained solid was filtered and dried *in vacuo* to give **29a** (28 mg, 17%) as a pale yellow solid. ^{1}H NMR (DMSO-d_6): δ 1.28 (3H, t, J = 7.4 Hz), 2.85 (2H, q, J = 7.5 Hz), 3.23 (3H, s), 7.55–7.68 (2H, m), 7.89–7.99 (1H, m), 8.13 (1H, s), 8.21–8.27 (1H, m),

8.29–8.40 (1H, m), 11.49 (1H, s); MS (ESI) *m/z* $[M+H]^+$ 355.

5-Chloro-3-[3-(methanesulfonyl)anilino]pyrazine-2-carboxamide (**29b**)

A mixture of 3,5-dichloropyrazine-2-carboxamide (**28b**, 450 mg, 2.34 mmol), 3-(methanesulfonyl)aniline (441 mg, 2.58 mmol), DIPEA (408 μL, 2.34 mmol) and 1,4-dioxane (20 mL) was stirred at 110 °C for 60 h. After the mixture was cooled, water was added, and the resulting slurry was extracted with EtOAc. The organic layer was dried over anhydrous $MgSO_4$, and concentrated *in vacuo*. The residue was purified by silica gel column chromatography ($CHCl_3$/MeOH = 100:0 to 50:1). The resulting product was washed with EtOAc to give **29b** (425 mg, 55%) as a pale yellow solid. ^{1}H NMR (DMSO-d_6): δ 3.24 (3H, s), 7.55–7.77 (2H, m), 7.90–8.04 (1H, m), 8.06–8.36 (3H, m), 8.50 (1H, s), 11.73 (1H, s); MS (FAB) *m/z* $[M+H]^+$ 327.

5-Chloro-3-[3-(methanesulfonyl)anilino]-6-propylpyrazine-2-carboxamide (**29c**)

A mixture of 3,5-dichloro-6-propylpyrazine-2-carboxamide (**28c**, 800 mg, 3.42 mmol), 3-(methanesulfonyl)aniline (644 mg, 3.76 mmol), DIPEA (596 μL, 3.42 mmol) and 1,4-dioxane (8 mL) in a sealed tube was stirred at 170 °C for 40 h and at 180 °C for 40 h. After the mixture was cooled, water was added, and the resulting slurry was extracted with EtOAc. The organic layer was dried over anhydrous $MgSO_4$ and concentrated *in vacuo*. The residue was purified by silica gel column chromatography ($CHCl_3$/MeOH = 100:0 to 30:1). The resulting product was

washed with EtOAc and the obtained solid was filtered and dried to give **29c** (581 mg, 46%) as a yellow solid. ^{1}H NMR (DMSO-d_6): δ 0.96 (3H, t, J = 7.3 Hz), 1.71–1.83 (2H, m), 2.76–2.86 (2H, m), 3.23 (3H, s), 7.56–7.61 (1H, m), 7.61–7.68 (1H, m), 7.89–7.98 (1H, m), 8.06–8.16 (1H, m), 8.22–8.26 (1H, m), 8.29–8.38 (1H, m), 11.48 (1H, s); MS (ESI) *m/z* $[M+H]^+$ 369, 371.

6-Ethyl-5-{[(1*r*,4*r*)-4-hydroxycyclohexyl]amino}-3-[3-(methanesulfonyl)anilino]pyrazine-2-carboxamide (**30a**)

A mixture of 5-chloro-6-ethyl-3-[3-(methanesulfonyl)anilino]pyrazine-2-carboxamide (**29a**, 140 mg, 0.395 mmol), (1*r*,4*r*)-4-aminocyclohexan-1-ol (364 mg, 3.16 mmol) and NMP (0.6 mL) was irradiated with microwaves at 190 °C for 30 min. After the mixture was cooled, EtOAc and water were added and the mixture was stirred for 30 min. The resulting solid was filtered. The solid was recrystallized from EtOH/H_2O to give **30a** (108 mg, 63%) as a white solid. ^{1}H NMR (DMSO-d_6): δ 1.19 (3H, t, J = 7.4 Hz), 1.31–1.51 (4H, m), 1.76–1.97 (4H, m), 2.60 (2H, q, J = 7.5 Hz), 3.21 (3H, s), 3.35–3.49 (1H, m), 3.87–4.03 (1H, m), 4.52 (1H, d, J = 4.4 Hz), 6.75 (1H, d, J = 7.6 Hz), 7.37 (1H, d, J = 2.4 Hz), 7.44–7.57 (2H, m), 7.61 (1H, d, J = 2.8 Hz), 7.96–8.04 (1H, m), 8.15–8.22 (1H, m), 11.58 (1H, s); MS (ESI) *m/z* $[M+H]^+$ 434; HRMS (ESI) *m/z* Calcd for $C_{20}H_{28}N_5O_4S$ $[M+H]^+$: 434.1857, Found: 434.1856.

5-{[(1*r*,4*r*)-4-Hydroxycyclohexyl]amino}-3-[3-(methanesulfonyl)anilino]pyrazine-2-

carboxamide (**30b**)

A mixture of 5-chloro-3-[3-(methanesulfonyl)anilino]pyrazine-2-carboxamide (**29b**, 150 mg, 0.459 mmol), (1*r*,4*r*)-4-aminocyclohexan-1-ol (264 mg, 2.29 mmol) and NMP (1 mL) was irradiated with microwaves at 190 °C for 10 min. After the mixture was cooled, saturated aqueous $NaHCO_3$ solution was added, and the resulting slurry was extracted with EtOAc. The organic layer was washed with brine, dried over anhydrous $MgSO_4$, and concentrated *in vacuo*. The residue was purified by silica gel column chromatography ($CHCl_3$/MeOH = 100:0 to 30:1). The resulting product was washed with heated EtOAc to give **30b** (156 mg, 84%) as a white solid. ^{1}H NMR (DMSO-d_6): δ 1.17–1.49 (4H, m), 1.73–1.89 (2H, m), 1.89–2.04 (2H, m), 3.21 (3H, s), 3.36–3.51 (1H, m), 3.73–3.91 (1H, m), 4.53 (1H, d, J = 4.0 Hz), 7.28–7.36 (1H, m), 7.39 (1H, s), 7.47–7.59 (2H, m), 7.65 (1H, d, J = 7.6 Hz), 7.70–7.79 (1H, m), 7.84–7.98 (1H, m), 8.35 (1H, s), 11.81 (1H, s); MS (ESI) *m/z* $[M+H]^+$ 406; HRMS (ESI) *m/z* Calcd for $C_{18}H_{24}N_5O_4S$ $[M+H]^+$: 406.1544, Found: 406.1542.

5-{[(1*r*,4*r*)-4-Hydroxycyclohexyl]amino}-3-[3-(methanesulfonyl)anilino]-6-propylpyrazine-2-carboxamide (**30c**)

Compound **30c** was prepared in 54% yield as a white solid from **29c** and (1*r*,4*r*)-4-aminocyclohexan-1-ol using a procedure similar to that described for **30a**. ^{1}H NMR (DMSO-d_6): δ 0.96 (3H, t, J = 7.4 Hz), 1.29–1.51 (4H, m), 1.60–1.74 (2H, m), 1.77–1.97 (4H, m), 2.57

(2H, t, *J* = 7.4 Hz), 3.21 (3H, s), 3.36–3.48 (1H, m), 3.87–4.03 (1H, m), 4.52 (1H, d, *J* = 4.4 Hz), 6.74 (1H, d, *J* = 8.0 Hz), 7.35 (1H, d, *J* = 2.8 Hz), 7.43–7.64 (3H, m), 7.95–8.03 (1H, m), 8.15–8.21 (1H, m), 11.57 (1H, s); MS (ESI) *m/z* $[M+H]^+$ 448; HRMS (ESI) *m/z* Calcd for $C_{21}H_{30}N_5O_4S$ $[M+H]^+$: 448.2013, Found: 448.2014.

5-{[(1*r*,4*r*)-4-Hydroxycyclohexyl]amino}-3-[3-(methanesulfonyl)anilino]-6-methylpyrazine-2-carboxamide (**30d**)

A mixture of 3,5-dichloro-6-methylpyrazine-2-carboxamide (**28d**, 61 mg, 0.296 mmol), 3-(methanesulfonyl)aniline (56 mg, 0.327 mmol), DIPEA (51 μL, 0.293 mmol) and 1,4-dioxane (20 mL) in a sealed tube was stirred at 170 °C for 40 h. After the mixture was cooled, saturated aqueous $NaHCO_3$ solution was added, and the resulting slurry was extracted with EtOAc. The organic layer was dried over $MgSO_4$ and concentrated *in vacuo*. To this residue were added 3-(methanesulfonyl)aniline (76 mg, 0.444 mmol) and DMI (1 mL), and the mixture was irradiated with microwaves at 220 °C for 1 h. To this reaction mixture was added (1*r*,4*r*)-4-aminocyclohexan-1-ol (171 mg, 1.48 mmol), and the mixture was irradiated with microwaves at 190 °C for 30 min. EtOAc was added to the reaction mixture, and the organic layer was washed with saturated aqueous $NaHCO_3$ solution and brine, dried over anhydrous $MgSO_4$, and concentrated *in vacuo*. The residue was purified by silica gel column chromatography ($CHCl_3$/MeOH = 100:0 to 30:1). The resulting product was washed with EtOAc to give **30d**

(38 mg, 31%) as a pale yellow solid. ^{1}H NMR (DMSO-d_6): δ 1.30–1.51 (4H, m), 1.75–1.98 (4H, m), 2.27 (3H, s), 3.21 (3H, s), 3.36–3.48 (1H, m), 3.87–4.00 (1H, m), 4.53 (1H, d, J = 4.4 Hz), 6.72 (1H, d, J = 8.0 Hz), 7.33 (1H, d, J = 2.0 Hz), 7.44–7.58 (2H, m), 7.68 (1H, d, J = 2.4 Hz), 7.95–8.03 (1H, m), 8.16–8.22 (1H, m), 11.60 (1H, s); MS (ESI) *m/z* $[M+H]^+$ 420; HRMS (ESI) *m/z* Calcd for $C_{19}H_{26}N_5O_4S$ $[M+H]^+$: 420.1700, Found: 420.1697.

6-Bromo-5-{[(1*r*,4*r*)-4-hydroxycyclohexyl]amino}-3-[3-(methanesulfonyl)anilino]pyrazine-2-carboxamide (**31**)

To a mixture of 5-{[(1*r*,4*r*)-4-hydroxycyclohexyl]amino}-3-[3-(methanesulfonyl)anilino]pyrazine-2-carboxamide (**30b**, 150 mg, 0.370 mmol), $CHCl_3$ (40 mL) and MeCN (20 mL) was added NBS (69 mg, 0.39 mmol), and the reaction mixture was stirred at room temperature for 2 h. To this reaction mixture was added silica gel, and the mixture was concentrated *in vacuo*. The residue was purified by silica gel column chromatography ($CHCl_3$/MeOH = 100:0 to 10:1) and the resulting product was washed with EtOAc to give **31** (130 mg, 73%) as a pale yellow solid. ^{1}H NMR (DMSO-d_6): δ 1.28–1.44 (2H, m), 1.44–1.60 (2H, m), 1.73–1.93 (4H, m), 3.22 (3H, s), 3.34–3.48 (1H, m), 3.84–3.99 (1H, m), 4.53 (1H, d, J = 4.0 Hz), 6.84 (1H, d, J = 8.4 Hz), 7.50 (1H, s), 7.53–7.61 (2H, m), 7.67 (1H, s), 7.90–7.99 (1H, m), 8.15–8.22 (1H, m), 11.68 (1H, s); MS (ESI) *m/z* $[M+H]^+$ 484, 486; HRMS (ESI) *m/z* Calcd for $C_{18}H_{23}BrN_5O_4S$ $[M+H]^+$: 484.0649, Found: 484.0650.

6-Cyclopropyl-5-{[(1*r*,4*r*)-4-hydroxycyclohexyl]amino}-3-[3-(methanesulfonyl)anilino]pyrazine-2-carboxamide (**32**)

A mixture of 6-bromo-5-{[(1*r*,4*r*)-4-hydroxycyclohexyl]amino}-3-[3-(methanesulfonyl)anilino]pyrazine-2-carboxamide (**31**, 50 mg, 0.103 mmol), cyclopropylboronic acid (18 mg, 0.210 mmol), $Pd(PPh_3)_4$ (24 mg, 0.021 mmol), K_2CO_3 (71 mg, 0.514 mmol), 1,4-dioxane (2.5 mL) and water (0.5 mL) was stirred at 100 °C for 3 h, then at 115 °C overnight. After the mixture was cooled to room temperature, saturated aqueous $NaHCO_3$ solution was added, and the resulting slurry was extracted with $CHCl_3$. The organic layer was washed with brine, dried, and concentrated *in vacuo*. The residue was purified by silica gel column chromatography ($CHCl_3$/MeOH/28% aqueous NH_3 = 100:0:0 to 100:10:1). The resulting product was treated with EtOAc and *n*-hexane, and filtered to give **32** (9.8 mg, 21%) as a yellow solid. ^{1}H NMR (DMSO-d_6): δ 0.80–0.89 (2H, m), 0.91–0.97 (2H, m), 1.30–1.54 (4H, m), 1.76–2.04 (4H, m), 2.06–2.19 (1H, m), 3.21 (3H, s), 3.36–3.49 (1H, m), 3.90–4.04 (1H, m), 4.53 (1H, d, J = 4.0 Hz), 7.00 (1H, d, J = 8.0 Hz), 7.31 (1H, d, J = 2.5 Hz), 7.43–7.69 (3H, m), 7.97–8.05 (1H, m), 8.14–8.18 (1H, m), 11.60 (1H, s); MS (ESI) *m/z* $[M+H]^+$ 446; HRMS (ESI) *m/z* Calcd for $C_{21}H_{28}N_5O_4S$ $[M+H]^+$: 446.1857, Found: 446.1856.

6-Chloro-5-{[(1*r*,4*r*)-4-hydroxycyclohexyl]amino}-3-[3-

(methanesulfonyl)anilino]pyrazine-2-carboxamide (**33**)

To a mixture of 5-{[(1*r*,4*r*)-4-hydroxycyclohexyl]amino}-3-[3-(methanesulfonyl)anilino]pyrazine-2-carboxamide (**30b**, 298 mg, 0.735 mmol), $CHCl_3$ (40 mL) and MeCN (10 mL) was added NCS (108 mg, 0.809 mmol), and the reaction mixture was stirred at 70 °C for 8 h. After the mixture was cooled, silica gel was added, and the mixture was concentrated *in vacuo*. The residue was purified by silica gel column chromatography. The resulting product was solidified from $CHCl_3$ and the solid was filtered. The obtained solid was washed with heated EtOAc to give **33** (189 mg, 58%) as a white solid. ^{1}H NMR (DMSO-d_6): δ 1.27–1.61 (4H, m), 1.74–1.95 (4H, m), 3.22 (3H, s), 3.34–3.48 (1H, m), 3.84–4.01 (1H, m), 4.53 (1H, d, J = 4.0 Hz), 7.17 (1H, d, J = 8.0 Hz), 7.49 (1H, s), 7.52–7.62 (2H, m), 7.68 (1H, s), 7.90–7.99 (1H, m), 8.18–8.24 (1H, m), 11.72 (1H, s); MS (ESI) *m/z* $[M+H]^+$ 440; HRMS (ESI) *m/z* Calcd for $C_{18}H_{23}ClN_5O_4S$ $[M+H]^+$: 440.1154, Found: 440.1155.

5-Chloro-6-ethyl-3-{2-methoxy-4-[4-(4-methylpiperazin-1-yl)piperidin-1-yl]anilino}pyrazine-2-carboxamide (**34**)

A mixture of 3,5-dichloro-6-ethylpyrazine-2-carboxamide (**28a**, 503 mg, 2.29 mmol), 2-methoxy-4-[4-(4-methylpiperazin-1-yl)piperidin-1-yl]aniline (**3a**, 699 mg, 2.30 mmol), DIPEA (0.78 mL, 4.56 mmol) and 1,4-dioxane (10 mL) was stirred at 110 °C for 25 h. After the mixture was cooled to room temperature, saturated aqueous $NaHCO_3$ solution was added,

and the resulting slurry was extracted with $CHCl_3$. The organic layer was washed with brine, dried over anhydrous $MgSO_4$, and concentrated *in vacuo*. The residue was purified by silica gel column chromatography ($CHCl_3$/MeOH/28% aqueous NH_3 = 100:0:0 to 90:9:1). The resulting product was washed with EtOAc, filtered and dried *in vacuo* at 50 °C to give **34** (701 mg, 63%) as an orange solid. ^{1}H NMR (DMSO-d_6): δ 1.25 (3H, t, J = 7.4 Hz), 1.43–1.59 (2H, m), 1.77–1.91 (2H, m), 2.14 (3H, s), 2.20–2.72 (11H, m), 2.79 (2H, q, J = 7.5 Hz), 3.64–3.75 (2H, m), 3.85 (3H, s), 6.51 (1H, dd, J = 2.4, 8.8 Hz), 6.65 (1H, d, J = 2.4 Hz), 7.83 (1H, d, J = 1.6 Hz), 8.04 (1H, d, J = 8.8 Hz), 8.12 (1H, d, J = 1.6 Hz), 11.11 (1H, s); MS (ESI) *m/z* $[M+H]^+$ 488.

6-Ethyl-5-{[(1*r*,4*r*)-4-hydroxycyclohexyl]amino}-3-{2-methoxy-4-[4-(4-methylpiperazin-1-yl)piperidin-1-yl]anilino}pyrazine-2-carboxamide (**35**)

A mixture of 5-chloro-6-ethyl-3-{2-methoxy-4-[4-(4-methylpiperazin-1-yl)piperidin-1-yl]anilino}pyrazine-2-carboxamide (**34**, 106 mg, 0.217 mmol), (1*r*,4*r*)-4-aminocyclohexan-1-ol (124 mg, 1.08 mmol) and NMP (2 mL) was irradiated with microwaves at 190 °C for 1 h. To the mixture was added saturated aqueous $NaHCO_3$ solution, and the resulting slurry was extracted with EtOAc. The organic layer was washed with brine, dried over anhydrous $MgSO_4$, and concentrated *in vacuo*. The residue was purified by silica gel column chromatography ($CHCl_3$/MeOH/28% aqueous NH_3 = 100:0:0 to 90:9:1). The resulting product was washed with EtOAc, filtered and dried *in vacuo* at 50 °C to give **35** (45 mg, 37%) as an ocher solid. ^{1}H NMR

(DMSO-d_6): δ 1.17 (3H, t, J = 7.4 Hz), 1.21–1.61 (6H, m), 1.78–2.04 (6H, m), 2.14 (3H, s), 2.19–2.72 (13H, m), 3.35–3.49 (1H, m), 3.56–3.69 (2H, m), 3.72–3.89 (1H, m), 3.83 (3H, s), 4.59 (1H, d, J = 4.8 Hz), 6.40 (1H, dd, J = 2.4, 9.2 Hz), 6.60 (1H, d, J = 7.6 Hz), 6.63 (1H, d, J = 2.8 Hz), 6.99 (1H, d, J = 2.4 Hz), 7.41 (1H, d, J = 2.0 Hz), 8.26–8.35 (1H, m), 11.02 (1H, s); MS (ESI) *m/z* $[M+H]^+$ 567; HRMS (ESI) *m/z* Calcd for $C_{30}H_{47}N_8O_3$ $[M+H]^+$: 567.3766, Found: 567.3765.

5-Chloro-6-ethyl-3-{3-methoxy-4-[4-(4-methylpiperazin-1-yl)piperidin-1-yl]anilino}pyrazine-2-carboxamide (**36**)

A mixture of 3,5-dichloro-6-ethylpyrazine-2-carboxamide (**28a**, 90 mg, 0.409 mmol), 3-methoxy-4-[4-(4-methylpiperazin-1-yl)piperidin-1-yl]aniline (**6**, 124 mg, 0.407 mmol), DIPEA (71 μL, 0.408 mmol) and 1,4-dioxane (3.6 mL) was stirred at 110 °C for 19 h. After the mixture was cooled, water was added, and the resulting slurry was extracted with EtOAc. The organic layer was dried over Na_2SO_4, and concentrated *in vacuo*. The residue was purified by silica gel column chromatography ($CHCl_3$/MeOH) to give **36** (110 mg, 55%) as an ocher solid. ^{1}H NMR ($CDCl_3$): δ 1.28 (3H, t, J = 7.4 Hz), 1.72–1.99 (4H, m), 2.29 (3H, s), 2.34–2.78 (11H, m), 2.85 (2H, q, J = 7.5 Hz), 3.44–3.59 (2H, m), 3.89 (3H, s), 5.38–5.57 (1H, m), 6.90 (1H, d, J =8.4 Hz), 7.08–7.19 (1H, m), 7.32–7.41 (1H, m), 7.62–7.80 (1H, m), 10.66 (1H, s); MS (ESI) *m/z* $[M+H]^+$ 488, 490.

6-Ethyl-5-{[(1*r*,4*r*)-4-hydroxycyclohexyl]amino}-3-{3-methoxy-4-[4-(4-methylpiperazin-1-yl)piperidin-1-yl]anilino}pyrazine-2-carboxamide (**37a**)

A mixture of 5-chloro-6-ethyl-3-{3-methoxy-4-[4-(4-methylpiperazin-1-yl)piperidin-1-yl]anilino}pyrazine-2-carboxamide (**36**, 150 mg, 0.307 mmol), (1*r*,4*r*)-4-aminocyclohexan-1-ol (175 mg, 1.52 mmol) and NMP (3 mL) was irradiated with microwaves at 190 °C for 60 min. After the mixture was cooled, saturated aqueous $NaHCO_3$ solution was added, and the resulting slurry was extracted with EtOAc. The organic layer was washed with brine, dried over anhydrous $MgSO_4$, and concentrated *in vacuo*. The residue was purified twice by silica gel column chromatography ($CHCl_3$/MeOH/28% aqueous NH_3 = 100:0:0 to 90:9:1). The resulting product was solidified from EtOAc, and the obtained solid was filtered and dried *in vacuo* at 50 °C to give **37a** (58 mg, 33%) as a yellow solid. ^{1}H NMR (DMSO-d_6): δ 1.17 (3H, t, J = 7.4 Hz), 1.20–1.31 (2H, m), 1.33–1.61 (4H, m), 1.72–1.96 (6H, m), 2.14 (3H, s), 2.17–2.61 (13H, m), 3.23–3.36 (2H, m), 3.36–3.48 (1H, m), 3.76–3.93 (1H, m), 3.81 (3H, s), 4.59 (1H, d, J = 4.4 Hz), 6.63 (1H, d, J = 7.6 Hz), 6.79 (1H, d, J = 8.8 Hz), 7.06 (1H, d, J = 2.4 Hz), 7.18 (1H, d, J = 2.8 Hz), 7.26 (1H, dd, J = 2.2, 8.6 Hz), 7.50 (1H, d, J = 2.8 Hz), 11.03 (1H, s); MS (ESI) *m/z* $[M+H]^+$ 567; HRMS (ESI) *m/z* Calcd for $C_{30}H_{47}N_8O_3$ $[M+H]^+$: 567.3766, Found: 567.3765.

***rac*-6-Ethyl-5-{[(1*R*,2*R*)-2-hydroxycyclohexyl]amino}-3-{3-methoxy-4-[4-(4-**

methylpiperazin-1-yl)piperidin-1-yl]anilino}pyrazine-2-carboxamide (**37b**)

A mixture of 5-chloro-6-ethyl-3-{3-methoxy-4-[4-(4-methylpiperazin-1-yl)piperidin-1-yl]anilino}pyrazine-2-carboxamide (**36**, 150 mg, 0.307 mmol), *rac*-(1*R*,2*R*)-2-aminocyclohexan-1-ol monohydrochloride (140 mg, 0.921 mmol), DIPEA (164 μL, 0.921 mmol) and NMP (3 mL) was irradiated with microwaves at 190 °C for 60 min. After the mixture was cooled, water was added, and the resulting precipitate was filtered. The obtained solid was purified by silica gel column chromatography ($CHCl_3$/MeOH = 84:16) to give **37b** (61 mg, 35%) as a brown solid. ^{1}H NMR (DMSO-d_6): δ 1.05–1.32 (4H, m), 1.20 (3H, t, J = 7.5 Hz), 1.45–1.59 (2H, m), 1.59–1.74 (2H, m), 1.74–1.86 (2H, m), 1.86–2.04 (2H, m), 2.14 (3H, s), 2.18–2.67 (13H, m), 3.20–3.41 (2H, m), 3.48–3.61 (1H, m), 3.73–3.87 (1H, m), 3.82 (3H, s), 4.64 (1H, d, J = 5.0 Hz), 6.56 (1H, d, J = 7.5 Hz), 6.79 (1H, d, J = 8.5 Hz), 7.10–7.23 (3H, m), 7.48 (1H, d, J = 2.5 Hz), 11.03 (1H, s); MS (ESI) *m/z* $[M+H]^+$ 567; HRMS (ESI) *m/z* Calcd for $C_{30}H_{47}N_8O_3$ $[M+H]^+$: 567.3766, Found: 567.3768.

6-Ethyl-5-{[(1*r*,4*r*)-4-methoxycyclohexyl]amino}-3-{3-methoxy-4-[4-(4-methylpiperazin-1-yl)piperidin-1-yl]anilino}pyrazine-2-carboxamide (**37c**)

To a mixture of 5-chloro-6-ethyl-3-{3-methoxy-4-[4-(4-methylpiperazin-1-yl)piperidin-1-yl]anilino}pyrazine-2-carboxamide (**36**, 100 mg, 0.205 mmol) and NMP (1.5 mL) was added (1*r*,4*r*)-4-methoxycyclohexan-1-amine (106 mg, 0.820 mmol), and the mixture

was irradiated with microwaves at 200 °C for 30 min. After the mixture was cooled, saturated aqueous $NaHCO_3$ solution was added, and the resulting slurry was extracted with EtOAc. The organic layer was washed with brine, dried over anhydrous $MgSO_4$, and concentrated *in vacuo*. The residue was purified by silica gel column chromatography ($CHCl_3$/MeOH/28% aqueous NH_3 = 100:0:0 to 200:10:1). The resulting product was solidified from EtOAc, filtered and dried to give **37c** (62 mg, 52%) as a yellow solid. ^{1}H NMR (DMSO-d_6): δ 1.10–1.28 (2H, m), 1.18 (3H, t, J = 7.4 Hz), 1.33–1.63 (4H, m), 1.73–1.86 (2H, m), 1.89–2.00 (2H, m), 2.00–2.11 (2H, m), 2.14 (3H, s), 2.18–2.64 (11H, m), 2.56 (2H, q, J = 7.3 Hz), 3.05–3.19 (1H, m), 3.22–3.39 (2H, m), 3.26 (3H, s), 3.75–3.95 (1H, m), 3.80 (3H, s), 6.66 (1H, d, J = 7.6 Hz), 6.78 (1H, d, J = 8.4 Hz), 7.05 (1H, d, J = 2.4 Hz), 7.18 (1H, d, J = 2.8 Hz), 7.24 (1H, dd, J = 2.4, 8.8 Hz), 7.50 (1H, d, J = 2.8 Hz), 11.01 (1H, s); MS (ESI) *m/z* $[M+H]^+$ 581; HRMS (ESI) *m/z* Calcd for $C_{31}H_{49}N_8O_3$ $[M+H]^+$: 581.3922, Found: 581.3924.

6-Ethyl-3-{3-methoxy-4-[4-(4-methylpiperazin-1-yl)piperidin-1-yl]anilino}-5-[(propan-2-yl)amino]pyrazine-2-carboxamide (**37d**)

Compound **37d** was prepared in 54% yield as a yellow solid from **36** and propan-2-amine using a procedure similar to that described for **37c**. ^{1}H NMR (DMSO-d_6): δ 1.18 (3H, t, J = 7.4 Hz), 1.23 (6H, d, J = 6.4 Hz), 1.45–1.62 (2H, m), 1.72–1.86 (2H, m), 2.06–2.64 (11H, m), 2.14 (3H, s), 2.57 (2H, q, J = 7.3 Hz), 3.23–3.40 (2H, m), 3.79 (3H, s), 4.26–4.43 (1H, m),

6.71 (1H, d, J = 8.0 Hz), 6.81 (1H, d, J = 8.4 Hz), 6.97 (1H, dd, J = 2.4, 8.8 Hz), 7.18 (1H, d, J = 3.2 Hz), 7.40 (1H, d, J = 2.4 Hz), 7.50 (1H, d, J = 2.8 Hz), 11.13 (1H, s); MS (ESI) *m/z* $[M+H]^+$ 511; HRMS (ESI) *m/z* Calcd for $C_{27}H_{43}N_8O_2$ $[M+H]^+$: 511.3503, Found: 511.3504.

6-Ethyl-5-(ethylamino)-3-{3-methoxy-4-[4-(4-methylpiperazin-1-yl)piperidin-1-yl]anilino}pyrazine-2-carboxamide (**37e**)

Compound **37e** was prepared in 49% yield as a yellow solid from **36** and ethanamine using a procedure similar to that described for **37a**. ^{1}H NMR (DMSO-d_6): δ 1.19 (3H, t, J = 7.2 Hz), 1.19 (3H, t, J = 7.2 Hz), 1.46–1.60 (2H, m), 1.73–1.84 (2H, m), 2.14 (3H, s), 2.19–2.61 (11H, m), 2.55 (2H, q, J = 7.5 Hz), 3.26–3.38 (2H, m), 3.41–3.54 (2H, m), 3.79 (3H, s), 6.81 (1H, d, J = 8.5 Hz), 6.98 (1H, dd, J = 2.3, 8.8 Hz), 7.11 (1H, t, J = 5.5 Hz), 7.18 (1H, d, J = 3.0 Hz), 7.45 (1H, d, J = 2.5 Hz), 7.51 (1H, d, J = 3.0 Hz), 11.15 (1H, s); MS (ESI) *m/z* $[M+H]^+$ 497; HRMS (ESI) *m/z* Calcd for $C_{26}H_{41}N_8O_2$ $[M+H]^+$: 497.3347, Found: 497.3346.

6-Ethyl-5-[ethyl(methyl)amino]-3-{3-methoxy-4-[4-(4-methylpiperazin-1-yl)piperidin-1-yl]anilino}pyrazine-2-carboxamide (**37f**)

Compound **37f** was prepared in 54% yield as a yellow solid from **36** and *N*-methylethanamine using a procedure similar to that described for **37c**. ^{1}H NMR (DMSO-d_6): δ 1.17 (3H, t, J = 7.2 Hz), 1.22 (3H, t, J = 7.5 Hz), 1.45–1.60 (2H, m), 1.73–1.85 (2H, m), 2.14

(3H, s), 2.18–2.62 (11H, m), 2.71 (2H, q, J = 7.3 Hz), 3.01 (3H, s), 3.26–3.36 (2H, m), 3.43 (2H, q, J = 7.0 Hz), 3.79 (3H, s), 6.82 (1H, d, J = 8.5 Hz), 7.02 (1H, dd, J = 2.2, 8.8 Hz), 7.33 (1H, d, J = 2.0 Hz), 7.40 (1H, d, J = 2.5 Hz), 7.70 (1H, d, J = 2.5 Hz), 10.99 (1H, s); MS (ESI) *m/z* $[M+H]^+$ 511; HRMS (ESI) *m/z* Calcd for $C_{27}H_{43}N_8O_2$ $[M+H]^+$: 511.3503, Found: 511.3504.

In vitro kinase inhibitory assay

EML4–ALK variant 1 protein was isolated from Ba/F3 cells transformed with EML4–ALK. Kinase activity was measured using HTRF® KinEASE™-TK (Cisbio Bioassays, Codolet, France). The final concentration of ATP for EML4–ALK variant 1 protein was 100 μM.

In vitro cell growth assay

Ba/F3 cells transformed with EML4–ALK variant 1 were seeded in 384-well plates at 5×10^2 cells per well, and treated with various concentrations of compounds for 2 days. Cell viability was measured using alamarBlue® Cell Viability Reagent (Thermo Fisher Scientific Inc., Waltham, MA, U.S.A.).

In vivo antitumor test in the 3T3 xenograft model

All experiments were performed in accordance with the regulation of the Animal Ethics Committee of Astellas Pharma Inc.

EML4–ALK fusion protein variant 1 expressing 3T3 cells were subcutaneously inoculated into the flank of male Balb/c nude mice (Charles River Japan, Inc.) at 3×10^6 cells/0.1 mL/mouse. The compounds (**12a**, **37a**, and **37c**) were suspended in vehicle (0.5% methylcellulose solution) and administered orally at a dose of 10 mg/kg, once daily from Day 1 to Day 5 (the first day of administration was designated Day 1).

Body weight and tumor diameter were measured using a balance and calipers, respectively, and tumor volume was determined by calculating the volume of an ellipsoid using the formula: length×width^2×0.5.

The percent inhibition of tumor growth on the last day of the observation (Day 5) was calculated using the following formula:

100 × {1 − [(mean tumor volume of mice treated with each compound on Day 5) – (mean tumor volume of mice treated with each compound on Day 1)] / [(mean tumor volume of mice treated with vehicle on Day 5) – (mean tumor volume of mice treated with vehicle on Day 1)]}

When percent inhibition of tumor growth exceeded 100%, the percent of tumor regression was calculated using the following formula:

100 × [1 − (mean tumor volume of mice treated with each compound on Day 5) / (mean tumor volume of mice treated with each compound on Day 1)]

Aqueous solubility

Solubility of the test compounds was evaluated by the Japanese Pharmacopoeia 2nd fluid for disintegration test (JP2; pH = 6.8 buffer). DMSO stock solutions (10 mM) of the test compounds were prepared and added to JP2. The solutions were shaken at 1000 rpm at 25 °C under light-protected conditions for 20 h. Precipitates were filtered through a PVDF membrane filter (pore size 0.22 μm, MERCK) and the concentration (μM) of the compound in the filtrate was assayed by high-performance liquid chromatography (HPLC).

Permeability

Parallel artificial membrane permeability assay (PAMPA) was conducted using STARlet 8ch (Hamilton Robotics, Reno, NV). In this assay, a 'sandwich' is formed by a 96-well microtiter plate (pION Inc., Billerica, MA) and a 96-well filter plate (pION Inc.) such that each composite well is divided into two chambers, with the donor at the bottom and acceptor at the top, separated by a lipid (pION Inc.)-coated microfilter disc. DMSO stock solutions (10 mM) of the test compounds were added to a mixture of aqueous buffer (pH 6.5) and DMSO (9:1). The drug solutions were filtered through a 96-well filter plate (PVDF, Corning Inc., Corning, NY) and added to the donor compartments. The plates were sandwiched together and acceptor buffer (pH 7.4, pION Inc.) was added to the acceptor compartment. The sandwiched plates were incubated at room temperature for 2 h under saturated water vapor conditions. After

incubation, the amount of the test compounds in donor and acceptor compartments were assayed by HPLC. Permeability was calculated using PAMPA Evolution software (pION Inc.).

Molecular modeling

Docking calculations for **30a** and **37a** were performed on the crystal structure of ALK (PDB code: 2XB7 [36]). The protein-ligand complex was prepared using the Protein Preparation Wizard in Maestro 2017-1 [41] (Schrödinger, LLC, New York, NY, 2017) with the Impref Module to apply the appropriate side-chain protonation states, and to refine and minimize the structure. Docking grids were generated and defined based on the centroid of NVP-TAE684 in the ATP-binding site, incorporating hydrogen-bond constraints to the hinge region and hydrophobic region constraints. Ligand receptor docking was carried out using XP mode in Glide in Maestro 2017-1 [41] (Schrödinger, LLC, New York, NY, 2017). The top scoring pose, as assessed by the Glidescore, was employed for discussion. All molecular visualizations were produced by MOE [42].

Conclusion

Research that aimed to identify novel EML4–ALK inhibitors for the treatment of EML4–ALK-positive NSCLC led to the identification of compounds **12a** (ASP3026) and **37c**.

In Chapter 1, I described the synthesis and biological evaluation of 1,3,5-triazine derivatives. I also revealed the detailed SARs of 1,3,5-triazine derivatives based on computational modeling of compound **12a** with ALK. Structure optimization of each component of 1,3,5-triazine derivative compounds led to the identification of compound **12a**. Once-daily oral administration of **12a** for 14 days demonstrated dose-dependent antitumor activity and induced tumor regression in mice xenografted with NCI-H2228, human NSCLC tumor cells expressing EML4–ALK.

In Chapter 2, I described the synthesis and biological evaluation of pyrazine-2-carboxamide derivatives to obtain a more potent EML4–ALK inhibitor with a different chemical structure to that of **12a**. I also revealed the detailed SARs of pyrazine-2-carboxamide derivatives based on computational modeling of compounds **30a** and **37a** with ALK. Structure optimization of each component of pyrazine-2-carboxamide derivative compounds led to the identification of compound **37c**. Once-daily oral administration of **37c** at a dose of 10 mg/kg for 5 days induced tumor regression by 62% in mice xenografted with 3T3 cells expressing EML4–ALK, which was more potent than that observed for **12a**.

In conclusion, compounds **12a** and **37c** were discovered as novel EML4–ALK inhibitors. These compounds may contribute to more profound understanding of the biology of EML4–ALK. Through this research, compounds that could lead to molecular targeted therapy for the treatment of EML4–ALK-positive NSCLC have been found.

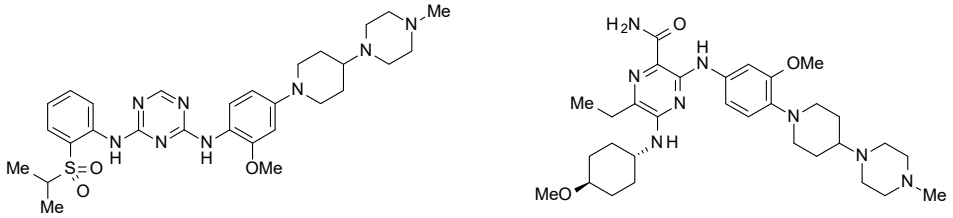

12a (ASP3026) **37c**

Figure 13. Structures of **12a** (ASP3026) and **37c**.

Acknowledgements

I would like to express my sincere gratitude to Specially Appointed Professor Hiroshi Nagase for his guidance and valuable discussions throughout the doctoral program in life science innovation (T-LSI). I am also grateful to Professor Hiroyuki Ito, Professor Noriki Kutsumura, and Associate Professor Yusaku Miyamae for their helpful support and valuable advice during the preparation of my doctoral dissertation.

I would like to thank Dr. Noriyuki Masuda, Dr. Masaaki Hirano, Dr. Yuji Matsushima, Dr. Susumu Watanuki, and Professor Sosuke Miyoshi for their helpful support during my doctoral program. Further, I am very thankful to Dr. Itsuro Shimada for his continuous support and valuable discussions during the preparation of my doctoral dissertation.

Finally, I would like to thank my family for their helpful support throughout my doctoral program.

References

1. Ferlay J., Soerjomataram I., Dikshit R., Eser S., Mathers C., Rebelo M., Parkin D. M., Forman D., Bray F., Cancer incidence and mortality worldwide: Sources, methods and major patterns in GLOBOCAN 2012, *Int. J. Cancer*, **2015**, *136*, E359–E386.
2. American Cancer Society, Lung Cancer: https://www.cancer.org/cancer/lung-cancer.html, [accessed on June 29, 2019]
3. Sharma S. V., Settleman J., Oncogene addiction: setting the stage for molecularly targeted cancer therapy, *Genes Dev.*, **2007**, *21*, 3214–3231.
4. Reck M., Heigener D. F., Mok T., Soria J.-C., Rabe K. F., Management of non-small-cell lung cancer: recent developments, *Lancet*, **2013**, *382*, 709–719.
5. Morris S. W., Kirstein M. N., Valentine M. B., Dittmer K. G., Shapiro D. N., Saltman D. L., Look A. T., Fusion of a Kinase Gene, *ALK*, to a Nucleolar Protein Gene, *NPM*, in Non-Hodgkin's Lymphoma., *Science*, **1994**, *263*, 1281–1284.
6. Duyster J., Bai R.-Y., Morris S.W., Translocations involving anaplastic lymphoma kinase (ALK), *Oncogene*, **2001**, *20*, 5623–5637.
7. Chiarle R., Voena C., Ambrogio C., Piva R., Inghirami G., The anaplastic lymphoma kinase in the pathogenesis of cancer, *Nat. Rev. Cancer*, **2008**, *8*, 11–23.
8. Mossé Y. P., Wood A., Maris J. M., Inhibition of ALK Signaling for Cancer Therapy, *Clin.*

Cancer Res., **2009**, *15*, 5609–5614.

9. Hallberg B., Palmer R. H., Mechanistic insight into ALK receptor tyrosine kinase in human cancer biology, *Nat. Rev. Cancer*, **2013**, *13*, 685–700.
10. Soda M., Choi Y. L., Enomoto M., Takada S., Yamashita Y., Ishikawa S., Fujiwara S., Watanabe H., Kurashina K., Hatanaka H., Bando M., Ohno S., Ishikawa Y., Aburatani H., Niki T., Sohara Y., Sugiyama Y., Mano H., Identification of the transforming *EML4–ALK* fusion gene in non-small-cell lung cancer, *Nature*, **2007**, *448*, 561–566.
11. Pollmann M., Parwaresch R., Adam-Klages S., Kruse M.-L., Buck F., Heidebrecht H.-J., Human EML4, a novel member of the EMAP family, is essential for microtubule formation, *Exp. Cell Res*., **2006**, *312*, 3241–3251.
12. Soda M., Takada S., Takeuchi K., Choi Y. L., Enomoto M., Ueno T., Haruta H., Hamada T., Yamashita Y., Ishikawa Y., Sugiyama Y., Mano H., A mouse model for *EML4–ALK*-positive lung cancer, *Proc. Natl. Acad. Sci. U.S.A.*, **2008**, *105*, 19893–19897.
13. Mano H., Non-solid oncogenes in solid tumors: *EML4–ALK* fusion genes in lung cancer, *Cancer Sci.*, **2008**, *99*, 2349–2355.
14. Shaw A. T., Solomon B., Targeting Anaplastic Lymphoma Kinase in Lung Cancer, *Clin. Cancer Res.*, **2011**, *17*, 2081–2086.
15. Cui J. J., Tran-Dubé M., Shen H., Nambu M., Kung P.-P., Pairish M., Jia L., Meng J., Funk L., Botrous I., McTigue M., Grodsky N., Ryan K., Padrique E., Alton G., Timofeevski S.,

Yamazaki S., Li Q., Zou H., Christensen J., Mroczkowski B., Bender S., Kania R. S., Edwards M. P., Structure Based Drug Design of Crizotinib (PF-02341066), a Potent and Selective Dual Inhibitor of Mesenchymal–Epithelial Transition Factor (c-MET) Kinase and Anaplastic Lymphoma Kinase (ALK), *J. Med. Chem*., **2011**, *54*, 6342–6363.

16. Marsilje T. H., Pei W., Chen B., Lu W., Uno T., Jin Y., Jiang T., Kim S., Li N., Warmuth M., Sarkisova Y., Sun F., Steffy A., Pferdekamper A. C., Li A. G., Joseph S. B., Kim Y., Liu B., Tuntland T., Cui X., Gray N. S., Steensma R., Wan Y., Jiang J., Chopiuk G., Li J., Gordon W. P., Richmond W., Johnson K., Chang J., Groessl T., He Y.-Q., Phimister A., Aycinena A., Lee C. C., Bursulaya B., Karanewsky D. S., Seidel H. M., Harris J. L., Michellys P.-Y., Synthesis, Structure–Activity Relationships, and in Vivo Efficacy of the Novel Potent and Selective Anaplastic Lymphoma Kinase (ALK) Inhibitor 5-Chloro-*N*2-(2-isopropoxy-5-methyl-4-(piperidin-4-yl)phenyl)-*N*4-(2-(isopropylsulfonyl)phenyl)pyrimidine-2,4-diamine (LDK378) Currently in Phase 1 and Phase 2 Clinical Trials, *J. Med. Chem.*, **2013**, *56*, 5675–5690.

17. Shaw A. T., Kim D.-W., Mehra R., Tan D. S. W., Felip E., Chow L. Q. M., Camidge D. R., Vansteenkiste J., Sharma S., De Pas T., Riely G. J., Solomon B. J., Wolf J., Thomas M., Schuler M., Liu G., Santoro A., Lau Y. Y., Goldwasser M., Boral A. L., Engelman J. A., Ceritinib in *ALK*-Rearranged Non-Small-Cell Lung Cancer, *N. Engl. J. Med*., **2014**, *370*, 1189–1197.

18. Kinoshita K., Asoh K., Furuichi N., Ito T., Kawada H., Hara S., Ohwada J., Miyagi T., Kobayashi T., Takanashi K., Tsukaguchi T., Sakamoto H., Tsukuda T., Oikawa N., Design and synthesis of a highly selective, orally active and potent anaplastic lymphoma kinase inhibitor (CH5424802), *Bioorg. Med. Chem*., **2012**, *20*, 1271–1280.

19. Kodama T., Tsukaguchi T., Yoshida M., Kondoh O., Sakamoto H., Selective ALK inhibitor alectinib with potent antitumor activity in models of crizotinib resistance, *Cancer Lett*., **2014**, *351*, 215–221.

20. Huang W.-S., Liu S., Zou D., Thomas M., Wang Y., Zhou T., Romero J., Kohlmann A., Li F., Qi J., Cai L., Dwight T. A., Xu Y., Xu R., Dodd R., Toms A., Parillon L., Lu X., Anjum R., Zhang S., Wang F., Keats J., Wardwell S. D., Ning Y., Xu Q., Moran L. E., Mohemmad Q. K., Jang H. G., Clackson T., Narasimhan N. I., Rivera V. M., Zhu X., Dalgarno D., Shakespeare W. C., Discovery of Brigatinib (AP26113), a Phosphine Oxide-Containing, Potent, Orally Active Inhibitor of Anaplastic Lymphoma Kinase, *J. Med. Chem*., **2016**, *59*, 4948–4964.

21. Johnson T. W., Richardson P. F., Bailey S., Brooun A., Burke B. J., Collins M. R., Cui J. J., Deal J. G., Deng Y.-L., Dinh D., Engstrom L. D., He M., Hoffman J., Hoffman R. L., Huang Q., Kania R. S., Kath J. C., Lam H., Lam J. L., Le P. T., Lingardo L., Liu W., McTigue M., Palmer C. L., Sach N. W., Smeal T., Smith G. L., Stewart A. E., Timofeevski S., Zhu H., Zhu J., Zou H. Y., Edwards M. P., Discovery of (10*R*)-7-Amino-12-fluoro-2,10,16-

trimethyl-15-oxo-10,15,16,17-tetrahydro-*2H*-8,4-(metheno)pyrazolo[4,3-*h*][2,5,11]-benzoxadiazacyclotetradecine-3-carbonitrile (PF-06463922), a Macrocyclic Inhibitor of Anaplastic Lymphoma Kinase (ALK) and c-ros Oncogene 1 (ROS1) with Preclinical Brain Exposure and Broad-Spectrum Potency against ALK-Resistant Mutations, *J. Med. Chem*., **2014**, *57*, 4720–4744.

22. Elleraas J., Ewanicki J., Johnson T. W., Sach N. W., Collins M. R., Richardson P. F., Conformational Studies and Atropisomerism Kinetics of the ALK Clinical Candidate Lorlatinib (PF-06463922) and Desmethyl Congeners, *Angew. Chem. Int. Ed*., **2016**, *55*, 3590–3595.
23. Roskoski R. Jr., Anaplastic lymphoma kinase (ALK) inhibitors in the treatment of ALK-driven lung cancers, *Pharmacol. Res.*, **2017**, *117*, 343–356.
24. Katayama R., Drug resistance in anaplastic lymphoma kinase-rearranged lung cancer, *Cancer Sci*., **2018**, *109*, 572–580.
25. Galkin A. V., Melnick J. S., Kim S., Hood T. L., Li N., Li L., Xia G., Steensma R., Chopiuk G., Jiang J., Wan Y., Ding P., Liu Y., Sun F., Schultz P. G., Gray N. S., Warmuth M., Identification of NVP-TAE684, a potent, selective, and efficacious inhibitor of NPM-ALK, *Proc. Natl. Acad. Sci. U.S.A.*, **2007**, *104*, 270–275.
26. Mori M., Ueno Y., Konagai S., Fushiki H., Shimada I., Kondoh Y., Saito R., Mori K., Shindou N., Soga T., Sakagami H., Furutani T., Doihara H., Kudoh M., Kuromitsu S., The

Selective Anaplastic Lymphoma Receptor Tyrosine Kinase Inhibitor ASP3026 Induces Tumor Regression and Prolongs Survival in Non–Small Cell Lung Cancer Model Mice, *Mol. Cancer Ther.*, **2014**, *13*, 329–340.

27. Iikubo K., Kondoh Y., Shimada I., Matsuya T., Mori K., Ueno Y., Okada M., Discovery of *N*-{2-Methoxy-4-[4-(4-methylpiperazin-1-yl)piperidin-1-yl]phenyl}-*N*′-[2-(propane-2-sulfonyl)phenyl]-1,3,5-triazine-2,4-diamine (ASP3026), a Potent and Selective Anaplastic Lymphoma Kinase (ALK) Inhibitor, *Chem. Pharm. Bull*., **2018**, *66*, 251–262.
28. Kondoh Y., Iikubo K., Kuromitsu S., Shindo N., Soga T., Furutani T., Shimada I., Matsuya T., Kurosawa K., Kamikawa A., Mano H., Di(arylamino)aryl compound, Patent: WO 2009/008371, **2009**.
29. Kuntz K., Uehling D. E., Waterson A. G., Emmitte K. A., Stevens K., Shotwell J. B., Smith S. C., Nailor K. E., Salovich J. M., Wilson B. J., Cheung M., Mook R. A., Baum E. W., Moorthy G., Imidazopyridine kinase inhibitors, Patent: US 2008/0300242, **2008**.
30. Reitz A. B., Baxter E. W., Codd E. E., Davis C. B., Jordan A. D., Maryanoff B. E., Maryanoff C. A., McDonnell M. E., Powell E. T., Renzi M. J., Schott M. R., Scott M. K., Shank R. P., Vaught J. L., Orally Active Benzamide Antipsychotic Agents with Affinity for Dopamine D_2, Serotonin 5-HT_{1A}, and Adrenergic α_1 Receptors, *J. Med. Chem.*, **1998**, *41*, 1997–2009.
31. Arvanitis A. G., Gilligan P. J., Chorvat R. J., Cheeseman R. S., Christos T. E.,

Bakthavatchalam R., Beck J. P., Cocuzza A. J., Hobbs F. W., Wilde R. G., Arnold C., Chidester D., Curry M., He L., Hollis A., Klaczkiewicz J., Krenitsky P. J., Rescinito J. P., Scholfield E., Culp S., De Souza E. B., Fitzgerald L., Grigoriadis D., Tam S. W., Wong Y. N., Huang S.-M., Shen H. L., Non-Peptide Corticotropin-Releasing Hormone Antagonists: Syntheses and Structure−Activity Relationships of 2-Anilinopyrimidines and -triazines, *J. Med. Chem.*, **1999**, *42*, 805–818.

32. Courtin A., von Tobel H.-R., Auerbach G., Notizen zur Synthese von 2-Aminophenylsulfonen, *Helv. Chim. Acta*, **1980**, *63*, 1412–1419.
33. Beria I., Ballinari D., Bertrand J. A., Borghi D., Bossi R. T., Brasca M. G., Cappella P., Caruso M., Ceccarelli W., Ciavolella A., Cristiani C., Croci V., De Ponti A., Fachin G., Ferguson R. D., Lansen J., Moll J. K., Pesenti E., Posteri H., Perego R., Rocchetti M., Storici P., Volpi D., Valsasina B., Identification of 4,5-Dihydro-1*H*-pyrazolo[4,3-*h*]quinazoline Derivatives as a New Class of Orally and Selective Polo-Like Kinase 1 Inhibitors, *J. Med. Chem.*, **2010**, *53*, 3532–3551.
34. Tang R.-Y., Zhong P., Lin Q.-L., Sulfite-Promoted One-Pot Synthesis of Sulfides by Reaction of Aryl Disulfides with Alkyl Halides, *Synthesis*, **2007**, 85–91.
35. Mesaros E. F., Thieu T. V., Wells G. J., Zificsak C. A., Wagner J. C., Breslin H. J., Tripathy R., Diebold J. L., McHugh R. J., Wohler A. T., Quail M. R., Wan W., Lu L., Huang Z., Albom M. S., Angeles T. S., Wells-Knecht K. J., Aimone L. D., Cheng M., Ator M. A., Ott

G. R., Dorsey B. D., Strategies to Mitigate the Bioactivation of 2-Anilino-7-Aryl-Pyrrolo[2,1-*f*][1,2,4]triazines: Identification of Orally Bioavailable, Efficacious ALK Inhibitors, *J. Med. Chem.*, **2012**, *55*, 115–125.

36. Bossi R. T., Saccardo M. B., Ardini E., Menichincheri M., Rusconi L., Magnaghi P., Orsini P., Avanzi N., Borgia A. L., Nesi M., Bandiera T., Fogliatto G., Bertrand J. A., Crystal Structures of Anaplastic Lymphoma Kinase in Complex with ATP Competitive Inhibitors, *Biochemistry*, **2010**, *49*, 6813–6825.
37. Iikubo K., Kurosawa K., Matsuya T., Kondoh Y., Kamikawa A., Moritomo A., Iwai Y., Tomiyama H, Shimada I., Synthesis and structure–activity relationships of pyrazine-2-carboxamide derivatives as novel echinoderm microtubule-associated protein-like 4 (EML4)–anaplastic lymphoma kinase (ALK) inhibitors, *Bioorg. Med. Chem*., **2019**, *27*, 1683–1692.
38. Shimada I., Kurosawa K., Matsuya T., Iikubo K., Kondoh Y., Kamikawa A., Tomiyama H., Iwai Y., Diamino heterocyclic carboxamide compound, Patent: WO 2010/128659, **2010**.
39. Shimada I., Matsuya T., Kurosawa K., Iikubo K., Kamikawa A., Kuromitsu S., Shindou N., Futami T., Kawase T., Sano Y., Yamanaka A., Nishimura K., Asaumi M., Tomiyama H., Iwai Y., Arylaminoheterocyclic carboxamide compound, Patent: WO 2012/053606, **2012**.
40. Suzuki T., Onda K., Murakami T., Negoro K., Yahiro K., Maruyama T., Shimaya A., Ohta M., Novel nitrogen-containing heterocyclic derivatives or salts thereof, Patent: WO

00/76980, **2000**.

41. **Schrödinger Release 2017-1**: Maestro, Schrödinger, LLC, New York, NY, 2017.

42. *Molecular Operating Environment (MOE)*, 2016.08; Chemical Computing Group Inc., 1010 Sherbrooke St. West, Suite #910, Montreal, QC, Canada, H3A 2R7, **2016**.